

PL-TR-91-2295

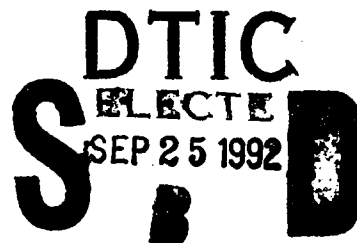
AD-A256 689



CLOUD SCENE SIMULATION MODELING

M.E. Cianciolo  
J.S. Hersh  
M.P. Ramos-Johnson

TASC  
55 Walkers Brook Drive  
Reading, Massachusetts 01867



20 November 1991

Scientific Report No. 1

Approved for Public Release, Distribution Unlimited

92 9 24 027

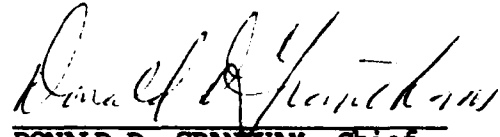
92-25803




PHILLIPS LABORATORY  
AIR FORCE SYSTEMS COMMAND  
HANSCOM AIR FORCE BASE, MASSACHUSETTS 01731-5000

"This technical report has been reviewed and is approved for publication"

  
BRUCE KUNKEL  
Contract Manager

  
DONALD D. GRANTHAM, Chief  
Atmospheric Structure Branch

  
ROBERT A. MCCLATCHEY, Director  
Atmospheric Sciences Division

This report has been reviewed by the ESD Public Affairs Office (PA) and is releasable to the National Technical Information Service (NTIS).

Qualified requestors may obtain additional copies from the Defense Technical Information Center.

If your address has changed, or if you wish to be removed from the mailing list, or if the addressee is no longer employed by your organization, please notify PL/IMA, Hanscom AFB, MA 01731-5000. This will assist us in maintaining a current mailing list.

Do not return copies of this report unless contractual obligations or notices on a specific document requires that it be returned.

# REPORT DOCUMENTATION PAGE

Form Approved  
OMB No. 0704-0188

Public reporting burden for this collection of information is estimated to average one hour per response, including the time for reviewing instructions, searching existing data sources, gathering and maintaining the data needed, and completing and reviewing the collection of information. Send comments regarding this burden estimate or any other aspect of this collection of information, including suggestions for reducing this burden, to Washington Headquarters Services, Directorate for Information Operations and Reports, 1215 Jefferson Davis Highway, Suite 1204, Arlington, VA 22202-4302, and to the Office of Management and Budget, Paperwork Reduction Project (0704-0188), Washington, DC 20503.

1. AGENCY USE ONLY (Leave blank)		2. REPORT DATE 20 November 1991		3. REPORT TYPE AND DATES COVERED Scientific No. 1	
4. TITLE AND SUBTITLE Cloud Scene Simulation Modeling				5. FUNDING NUMBERS PE 62101F PR 6670 TA 09 WU BE Contract F19628-90-C-0022	
6. AUTHOR(S) M.E. Cianciolo      M.P. Ramos-Johnson J.S. Hersh					
7. PERFORMING ORGANIZATION NAME(S) AND ADDRESS(ES) TASC 55 Walkers Brook Drive Reading, MA 01867				8. PERFORMING ORGANIZATION REPORT NUMBER	
9. SPONSORING/MONITORING AGENCY NAME(S) AND ADDRESS(ES) Phillips Laboratory Hanscom AFB, MA 01731-5000  Contract Manager: Donald Grantham/LYA				10. SPONSORING/MONITORING AGENCY REPORT NUMBER  PL-TR-91-2295	
11. SUPPLEMENTARY NOTES					
12a. DISTRIBUTION/AVAILABILITY STATEMENT Approved for public release; distribution unlimited				12b. DISTRIBUTION CODE	
13. ABSTRACT (Maximum 200 words)  This report documents the development of the Prototype and Interim versions of the Cloud Scene Simulation Model developed for Phillips Laboratory in support of the Smart Weapons Operability Enhancement Program under the Balanced Technology Initiative. The model simulates multi-dimensional cloud water density fields using stochastic field generation techniques (the sawtooth wave and successive random additions fractal algorithms) and knowledge of atmospheric structure for input to radiative transfer models and scene generation systems.  Two auxiliary post-processor programs are also described in this report. The first generates a two-dimensional shadow map from a cloud field as a function of solar position. The second, converts a gridded field to a colored polygonal isosurface for use in scene visualization.  Lastly, we include the results of a comparison of model produced and observed liquid water density statistics along paths through clouds of various types using data provided by the FAA. Plans for further model development (including the addition of a cumuliform model) are described.					
14. SUBJECT TERMS Cloud model      Liquid water density Sawtooth wave model      Scene simulation Fractal model      Isosurface algorithm				15. NUMBER OF PAGES 82	
				16. PRICE CODE	
17. SECURITY CLASSIFICATION OF REPORT Unclassified	18. SECURITY CLASSIFICATION OF THIS PAGE Unclassified	19. SECURITY CLASSIFICATION OF ABSTRACT Unclassified	20. LIMITATION OF ABSTRACT  SAR		

# TABLE OF CONTENTS

	Page
<b>LIST OF FIGURES</b>	<b>v</b>
<b>LIST OF TABLES</b>	<b>viii</b>
<b>1. INTRODUCTION</b>	<b>1</b>
1.1 Purpose Of The Project	1
1.2 Overview Of Project Tasks	1
<b>2. MODEL DESIGN AND IMPLEMENTATION</b>	<b>3</b>
2.1 Model Requirements And Design	3
2.2 The Prototype Model (Version 1.0)	6
2.2.1 Prototype Model Requirements and Design	6
2.2.2 Major Prototype Model Procedures	8
2.2.3 Results and Conclusions	26
2.3 The Interim Model (Version 2.0)	29
2.3.1 Interim Model Requirements and Design	29
2.3.2 Modifications Included In the Interim Model	31
2.3.3 Results And Conclusions	39
2.4 The Cloud Shadow Post-processor	41
2.4.1 Major Procedures	41
2.4.2 Methodology	43
2.5 The Visualization Post-processor	47
2.5.1 The Marching Cubes Algorithm	47
2.5.2 Assigning Colors To Cloud Surfaces	50
<b>3. STATISTICAL ANALYSIS OF CLOUD DATA</b>	<b>53</b>
3.1 Cloud Model Demonstration Sites	53
3.2 Faa Database Description	54
3.3 Spatial Series Data Selection	55
3.4 Comparison Of One-dimensional Spatial Series	65
<b>4. SUMMARY AND FUTURE PLANS</b>	<b>69</b>
4.1 Summary	69
4.2 The Enhanced Model (Version 3.0)	69

## TABLE OF CONTENTS (Continued)

	<b>Page</b>
4.3 Evaluation Of Field Algorithms	70
4.4 Integration With Other SWOE Models	70
<b>REFERENCES</b>	<b>72</b>

<b>Accession For</b>	
NTIS GRA&I	<input checked="" type="checkbox"/>
DTIC TAB	<input type="checkbox"/>
Unannounced	<input type="checkbox"/>
Justification	
By _____	
Distribution/	
Availability Codes	
<b>Dist</b>	Avail and/or Special
A-1	

DTIC QUALITY INSPECTED 3

## LIST OF FIGURES

Figure		Page
1	Cross-Sectional View of Sawtooth Wave (From Ref. 1)	10
2	Formation of Sawtooth Waves in Horizontal Domain (From Ref. 1)	10
3	Sequence of Binary Cloud Scenes (50% Cloud Cover, $50 \times 50$ km Horizontal Domain) Generated with the Two-Dimensional BSW Method with Differing Number of Waves	13
4	Sequence of Binary Cloud Scenes (50% Cloud Cover, $50 \times 50$ km Horizontal Domain) Generated with the Two-Dimensional BSW Method with Various Values for the Wavelength (in km)	14
5	Brownian Motion With Scale Factors Ranging from $r=1/8$ to $r=8$ Corresponding to Expanding and Contracting the Original Function Along the Horizontal Direction (From Ref. 3)	16
6	Fractional Brownian Motion With Various Values of the Hurst Parameter, Lacunarity Parameter = 0.5	17
7	Two Steps of the Midpoint Displacement Method	18
8	Fractional Brownian Motion with Various Values of the Lacunarity Parameter, Hurst Parameter = 0.7	19
9	Fundamental Structure Used in Dome-Building Process to Generate Upper Cloud Surface	20
10	Variables Used in Bilinear Interpolation (See Eq. 2.2-10)	21
11	Three-Dimensional Geometry Used in the BSW Method. All Points on the Plane ABC have Constant Wave Height. The line OP is the Shortest Distance from the Origin to the Plane and Has Angles $\alpha$ , $\beta$ , $\gamma$ with the x,y and z Axes (From Ref. 2)	23
12	Profile of Percent of Maximum Condensed Moisture for Sc and Ac Cloud Types Used in the Computation of Mean LWC for a Given Level in a Cloud Layer (From Ref. 7)	25
13	50% Stratus Cloud Layer Generated With the Prototype Model ( $20 \times 20$ km Horizontal Domain)	27
14	50% Stratus Cloud Layer Generated With the Prototype Model. Artifacts From the BSW Model are Clearly Visible	28
15	Series of Images Taken at Consecutive Stages in the Development of a Two-Dimensional Cloud Field Using the Method of Successive Random Additions ( $H=0.5$ , $r = 0.5$ )	33

## LIST OF FIGURES (Continued)

Figure		Page
16	Binary Cloud Field (50% Cloud Cover) Generated By Applying a Threshold Value to the Fractal Field of Fig. 15	34
17	Sequence of Binary Cloud Scenes (50% Cloud Cover) Generated with the Two-Dimensional SRA Method with Various Values for the Hurst Parameter ( $r = 0.5$ )	35
18	Sequence of Binary Cloud Scenes (50% Cloud Cover) Generated with the Two-Dimensional SRA Method with Various Values for the Lacunarity Parameter ( $H=0.5$ )	36
19	Binary Cloud Scenes (50% Cloud Cover, $10 \times 10$ km Horizontal Domain) Generated with the Two-Dimensional SRA Algorithms for Various Cloud Types	37
20	60% Stratus Cloud Layer Produced with the Interim Cloud Model	39
21	60% Stratocumulus Cloud Layer Produced with the Interim Cloud Model	40
22	60% Cirrus Cloud Layer Produced with the Interim Cloud Model	40
23	Relationship of Cloud and Ground Domains in the Cloud Shadow Post-Processor	42
24	X-Z Cross-Section Showing Variables Used in Cloud Shadow Calculations	44
25	Geometry Used to Convert Solar Angles to Cartesian Coordinates	45
26	Index Look-Up Table with Vertex Geometry Displayed for Reference (From Ref. 15)	48
27	The Fifteen Fundamental Polygonal Facet Representations. The Large Filled Circles Correspond to Points Within the Isosurface, and the Smaller Unfilled Circles Lie Outside the Isosurface (From Ref. 15)	49
28	Direction Vectors from Three Sample Vertices Through the Cloud Toward the Sun. Integrated Liquid Water Content Along each Vector is used in Color Computations	51
29	View From Below a 60% Stratocumulus Layer ( $10 \times 10$ km Horizontal Domain) Showing the Effects of Polygon Coloring with the Solar Azimuth and Zenith Angles Equal to $45^\circ$	52

## LIST OF FIGURES (Continued)

Figure	Page
30 Data Profile of All Cloud Types Measured in Northeastern California During February to March 1979-1983	56
31 Data Profile of Stratus (St) Clouds Measured in Northeastern California During February to March 1979-1983	58
32 Data Profile of Stratocumulus (Sc) Clouds Measured in Northeastern California During February to March 1979-1983	59
33 Data Profile of Cumulus (Cu) Clouds Measured in Northeastern California During February to March 1979-1983	60
34 Data Profile of Towering Cumulus (Tc) Clouds Measured in Northeastern California During February to March 1979-1983	61
35 Data Profile of Orographic Cumulus (Orcu) Clouds Measured in Northeastern California During February to March 1979-1983	62
36 Data Profile of Orographic Stratocumulus (Orsc) Clouds Measured in Northeastern California During February to March 1979-1983	63
37 Sample Scatter Plots Used in Data Selection Process (This Example For Orcu Cloud Type). Datasets with Longest Duration at Various ALWC and Altitude Values were Selected	64
38 Observed (using FSSP) and Corresponding Modeled LWC Spatial Series for Orsc and St Cloud Types	66
39 Autocorrelation Functions for the LWC Spatial Series in Fig. 38	67



## LIST OF TABLES

Table		Page
1	Overall SWOE Requirements	4
2	Requirements and Design for Prototype Model	7
3	The Maximum Condensed Moisture (in g/m <sup>3</sup> ) that can Occur in a Nonprecipitating Cloud as a Function of Cloud Type and Temperature (From Ref. 7). Cloud Types Simulated in the Prototype Model are Highlighted	24
4	Requirements and Design for Interim Model	30
5	Default Values for the Hurst and Lacunarity Parameters Used in the Generation of the Horizontal Cloud/No Cloud Field for Various Cloud Types	38

# **1. INTRODUCTION**

## **1.1 PURPOSE OF THE PROJECT**

One goal of the Smart Weapon Operability Enhancement (SWOE) Program under the Balanced Technology Initiative (BTI) is to enhance the operational capabilities of future smart weapons through more comprehensive consideration of the environment. A key element of the SWOE program is a planned sensor evaluation and test facility for millimeter wave (MMW) and infrared (IR) sensors. Sensor studies will be carried out using both actual field data and simulated data. The purpose of the Cloud Scene Model Development project is to meet the latter objective by simulating realistic cloud fields for use in radiometric sensor evaluation studies as well as scene visualization. Two major efforts of the Cloud Scene Simulation project are model software development and applied research.

## **1.2 OVERVIEW OF PROJECT TASKS**

Model software development tasks include the design, implementation, integration, testing, documentation and delivery of two interim models and a final cloud model. Applied research tasks include the analysis of cloud data (specifically liquid water density) and the comparison of various synthetic field generation techniques. Results from these analyses are used in model development with the goal of producing physically and visually realistic cloud fields with computational efficiency.

The six technical tasks are outlined below. Further detail on the tasks completed to date (Tasks 1 through 4) follows in Sections 2 and 3 of this report. Future tasks are discussed in Section 4.

### **TASK 1 MODEL DESIGN**

Analyze SWOE requirements. Design a stochastic cloud scene simulation model based on observed cloud morphology and atmospheric physics. Specify algorithms, data structures, data flows and software architecture.

### **TASK 2 MODEL VERSION 1.0 (The Prototype Model)**

Rapidly implement, test and deliver a prototype cloud model based on the Boehm sawtooth wave technique for generation of random fields (Refs. 1 and 2). Model stratiform cloud type only. Test software before delivery. Prepare a User's Guide.

### **TASK 3 STUDIES AND ANALYSES**

Survey recent scientific literature to identify prior investigations of the spatial and temporal variability of cloud water over geographical regions of interest. If necessary, locate, obtain and analyze empirical cloud data. Compare alternate field generation algorithms including the Boehm sawtooth wave, fractional Brownian motion (Ref. 3) and the turning bands (Ref. 4) techniques. Determine model parameters which will result in shapes and water distributions characteristic of stratiform, cumuliform and cirriform cloud types.

### **TASK 4 MODEL VERSION 2.0 (The Interim Model)**

Refine the prototype model based on the results of Task 3. Add the capability to generate cirriform cloud types. Test prior to delivery. Prepare a User's Guide.

### **TASK 5 SWOE COMPATIBILITY**

Evaluate selected SWOE cloud history databases and radiative transfer models for compatibility with the cloud scene simulation model.

### **TASK 6 MODEL VERSION 3.0 (The Enhanced Model)**

Refine the interim model using the knowledge gained in previous tasks. Develop a cumuliform cloud model and add temporal dimension. Test software prior to delivery. Prepare a User's Guide.

## **2.**

## **MODEL DESIGN AND IMPLEMENTATION**

The development of the Cloud Scene Simulation model is an iterative process, consisting of requirements analysis, model design, implementation, testing and documentation. In this section we discuss the development of the prototype and interim models. We also describe two supporting software packages; the shadow post-processor which computes the ground shadow for a given location, time of day and cloud field, and the visualization post-processor which reduces the cloud model output to colored polygonal surfaces for use in scene visualization at the Engineer Topographic Laboratories.

### **2.1 MODEL REQUIREMENTS AND DESIGN**

Evaluation of SWOE requirements was the early focus of the Cloud Scene Simulation project, followed by model design. In discussions with other SWOE participants, including personnel at the Phillips Laboratory, a set of requirements was formulated. Those requirements are outlined in the left-hand column of Table 1. The right-hand column contains the model design decisions responding to each of the requirements.

One can imagine simulating cloud fields by many possible methods: approximating specific cloud types by simple geometric shapes, using a physics-based numerical weather model, generating fine structure cloud fields within coarse resolution nephanalysis-type data, or using one of various stochastic field generation techniques. Based on an analysis of the first four requirements listed in Table 1, we chose to base the cloud model on stochastic field generation techniques.

These techniques can provide an excellent tool for the generation of complex fields. Such fields are more representative of the complexity found in natural cloud fields than simple geometric representations (e.g., approximating a stratus layer with a flat plane). This is important for simulating sensor response to complex cloud edges, holes and other density variations. All of the stochastic algorithms we considered for this project allow the user to control the complexity in a field by varying parameters in the algorithm.

Given the range of domain sizes and resolutions required by the SWOE program, relatively efficient stochastic models are preferable to numerically intensive physical

**Table 1      Overall SWOE Requirements**

	<b>SWOE MODEL REQUIREMENTS</b>	<b>DESIGN DECISIONS</b>
1	Produce realistic spatial and temporal distributions of cloud water (for stratiform, cirriform and cumuliform types) in the absence of real data.	Use stochastic algorithm.
2	Treat the complex structures of clouds for realism in radiometric sensor computations (e.g., cloud edge effects).	
3	Generate multiple scenes given identical meteorological input for sensitivity studies.	
4	Produce cloud fields in a computationally efficient manner.	
5	Generate high resolution cloud fields where necessary for use in radiometric computations and visualization (accommodate low resolution clouds on the horizon).	Incorporate variable resolution data grid.
6	Allow for a wide range of ground domain sizes and resolutions.	Use variable resolution grid to economize on memory storage requirements and simulate scenes on scales of 10-100 km.
7	Provide capability to generate scenes for a variety of sensor applications (e.g., top down, skimmer, air-to-air, etc.).	Generate fields that can be viewed from all angles. Include capability to produce scenes large enough to have clouds stretching off to the horizon.
8	Produce cloud scenes representative of any user-specified location and historical time.	Accept historical meteorological data on model input.
9	Generate model output in a form that can be used for radiometric sensor studies (both MMW and IR applications).	Produce liquid water density fields as output.
10	Integrate model with other SWOE simulation models.	Design model with replaceable interface module. Write all software in standard FORTRAN 77. Design model to be highly modular.
11	Provide polygonalized cloud scenes to ETL for visualization.	Implement polygon generation method with the capability to simulate colored cloud scenes (for additional realism).
12	Generate cloud shadow map for input to energy balance computations.	Provide a cloud shadow post-processor.

models. Additionally, stochastic fields are ideally suited to multiple simulations and sensitivity studies. Given identical meteorological input, countless scenes can be generated (all satisfying the same scene requirements) by varying a random number seed used to initialize the stochastic model. Such sensitivity studies will be an integral part of radiometric sensor evaluation studies.

Requirements 5 through 7 listed in Table 1 concern the size, shape and resolution of the simulated cloud domain. By employing a variable resolution data structure, we can produce the high resolution necessary over the domain of interest (approximately 5-10 meters), as well as lower resolution away from the area (e.g., off to the horizon as required for the cloud shadow program). This type of variable resolution geometry is not only computationally efficient, but it mimics the way we view clouds: higher resolution overhead, stretching off to lower resolutions at the horizon. A variable resolution data structure was not implemented in either the prototype or interim model, but will be a part of the enhanced model.

A further requirement within the SWOE program is that the cloud model simulate fields representative (at least in a statistical sense) of specific locations and past times. It is important to note that the model is *not* required to simulate the exact location of clouds and distribution of liquid water on any given day, rather, the requirement is to simulate cloud fields that have representative mean, variance and spatial distribution of cloud water for the area and time of interest. Three locations have been proposed as demonstration sites including one each in California, Michigan and Germany. The cloud model will use historical meteorological data from these locations as input (e.g., temperature and humidity soundings, cloud base and top heights, etc.).

The ninth and tenth requirements listed in Table 1 concern integrating the cloud model with other SWOE models. First, cloud model output fields will be used as input to radiometric sensor studies. An evaluation of several radiative transfer models resulted in the conclusion that liquid water density data is sufficient information from which to compute radiative properties of the cloud field (Ref. 5). Second, we use standard FORTRAN 77 and a highly modular model design to simplify integration.

Finally, the last two requirements concern post-processing of the gridded liquid water content fields. We have designed the visualization and cloud shadow post-processors to satisfy these requirements. Both are discussed later in this report. Similar tables of

requirements and design decisions specific to the prototype and interim models follow in Sections 2.2.1 and 2.3.1, respectively.

## **2.2 THE PROTOTYPE MODEL (VERSION 1.0)**

TASC rapidly developed, tested and delivered a prototype cloud scene model based on the Boehm sawtooth wave (BSW) and fractional Brownian motion (FBM) stochastic field generation models. Both low and middle cloud layers can be generated with this model.

Two versions of the prototype model (differing only in their memory requirements) were delivered: a high resolution version intended to run on a workstation or mainframe computer, and a low resolution version designed for a PC. A description of the prototype model is provided in this section. Additional details about the prototype model, including software organization, model input and output and installation, can be found in the User's Guide (Ref. 6). Improvements to the prototype model have been included in the second version of the cloud model (the interim model) and are described in Section 2.3.

### **2.2.1 Prototype Model Requirements and Design**

Requirements specific to the development of the prototype model are described briefly in Table 2. Many of the design decisions listed in the table were direct results of the time constraints inherent in the development of a rapid prototype model. For example, because of TASC's previous experience with the technique, we chose the Boehm sawtooth wave algorithm to generate stochastic fields. By using the sawtooth wave model as a base, we were able to develop a cloud model quickly. Likewise, due to time constraints and the fact that scenes were to be generated at specific locations only (e.g., Hunter-Liggett, California), we decided to limit the prototype model capability to a small number of cloud types (stratus (St), stratocumulus (Sc), altostratus (As) and altocumulus (Ac)) and cloud layers (low and middle).

Due to the rapid development cycle, we chose to simulate cloud fields in three dimensions only. Temporal evolution will be included in the enhanced model. A regular 3-d Cartesian grid was used throughout the prototype and interim models as well. This resulted not only in more rapid development time, but in a more portable model for early users of the model.

**Table 2      Requirements and Design for Prototype Model**

	PROTOTYPE MODEL REQUIREMENTS	DESIGN DECISIONS
1	Develop quickly for feedback from other SWOE participants.	Use BSW stochastic field generation model.
		Limit to stratiform cloud types: St, Sc, As, Ac.
		Limit to two cloud layers: low and middle.
		Simulate cloud fields in three dimensions only. Do not simulate temporal dimension.
		Use a regular Cartesian grid.
2	Use standard and portable software for easy integration with other SWOE models.	Write software in standard FORTRAN 77. Rely on no system functions or computer-specific extensions. Write output files as ASCII files for easy portability. Use regular 3-d grid geometry.
3	Create stand-alone program.	Build interface routine which communicates with the user. Acquire input data from user by question and answer. Write field to output file for further processing.
		Generate temperature profile from user-specified surface temperature and known wet and dry adiabatic lapse rates. User specifies cloud type, base and top heights.
4	Develop model without complete knowledge of liquid water content distributions.	Assume Gaussian distribution of water with standard deviation equal to 10% of the mean.
5	Simulate cloud water fields representative of specific cloud types and environmental conditions.	Use mean liquid water content data (for given cloud type and temperature) from Feddes' AWS report (Ref. 7).
6	Simulate realistic 3-d structure of cloud types.	Use multi-step technique to produce overall field. Use BSW model to generate horizontal structure. Build vertical structure based on dome-like shape. Generate 3-d internal structure independently with separate model parameters.

The cloud model is only one element of the larger SWOE program. With this in mind, we carefully designed a robust and easily-removable driver for the model. All input parameters and output data are passed through this interface. Thus the cloud model acts as a "black box" which accepts various parameters as input and generates gridded cloud data as output. Input parameters include information about the environmental conditions



at a specific location and time (see Section 2.2.2 for a list of input parameters). Sounding data are not used in the prototype and interim models (though they will be used in the enhanced model). We therefore assumed a temperature profile based on standard dry and wet lapse rates outside and inside the cloud region, respectively.

To satisfy the fifth requirement listed in Table 2, to simulate cloud water fields representative of specific cloud types and conditions, we used a method described in Ref. 7 that defines the mean liquid water content for any vertical level within a cloud layer as a function of cloud type, temperature and vertical position within the layer. In both the prototype and interim models we assumed that liquid water could be modeled as having a Gaussian distribution with mean computed as in Ref. 7, and with constant coefficient of variation (we use 10%, as discussed in Section 2.2.2). Assumptions about means and distributional forms will be tested later in the Studies and Analyses task of this project (Task 3).

Most importantly, in response to the last requirement listed in Table 2, it was necessary to produce three-dimensional stochastic fields that reproduce the spatial characteristics of the four previously-mentioned cloud types. These cloud types (St, Sc, As, Ac) are known for their relatively flat cloud bases, characteristic of the isotropic horizontal temperature distributions within which they frequently form. They also have generally smooth, undulating upper cloud surfaces. Through TASC's experience with working with various stochastic field algorithms, it was thought that no single three-dimensional algorithm could replicate the specific horizontal and vertical structure of these clouds. Therefore the prototype model was designed as a multi-stage process. The two-dimensional Boehm sawtooth wave algorithm was used to generate the distribution of clouds in the horizontal. A fractal model was used to generate the vertical cloud structure. A three-dimensional field generation technique was used to generate the internal liquid water density variations. This combination provided a starting point for model development.

## **2.2.2 Major Prototype Model Procedures**

An outline of the major procedures in the prototype model is provided here. Each procedure is described in more detail in the following subsections.

- Acquire model input parameters
- Generate horizontal cloud field

- Generate upper cloud surface
- Generate lower cloud surface
- Generate internal cloud structure
- Write three-dimensional cloud field to output file.

*Acquire Model Input Parameters* — Various parameters are required as input to the prototype model. The user specifies cloud base and top heights (for each layer) along with horizontal range to define the overall cloud region. Fractional coverage and cloud type are also requested for each layer. Surface temperature and elevation are used to compute a temperature profile for the liquid water density computations. The remaining input parameters include grid resolution, random number seed and output filename.

*Generate Horizontal Cloud Field* — The BSW model, developed at the Phillips Laboratory, is used to generate the initial distribution of cloud elements in the horizontal plane. First a two-dimensional Gaussian field is generated. A threshold value is then applied to the field to define a binary cloud/no cloud distribution. Later, upper and lower surfaces are built around cloud elements to create a three-dimensional cloud scene. In this section we provide an overview of the procedure used to generate a horizontal cloud distribution. We begin with a brief review of the BSW model. A more thorough description of the model can be found in Ref. 1.

The BSW model generates a Gaussian perturbation field. The field is generated by superimposing multiple “sawtooth waves” onto the horizontal domain, summing the heights of the sawtooth waves at each grid point in the domain and normalizing the resulting height. The sawtooth waves are stationary waves with specified wavelength (for our application, wavelength is a function of cloud type). The wave height varies linearly from 0 to 1 across the length of the wave. A cross-sectional view of the sawtooth wave is shown in Fig. 1. Multiple (N) waves with random orientation and phase (as measured from the center of the horizontal domain) are overlaid across the two-dimensional space. The three parameters defining the sawtooth waves and their geometric relationship to the horizontal cloud domain are shown in Fig. 2.

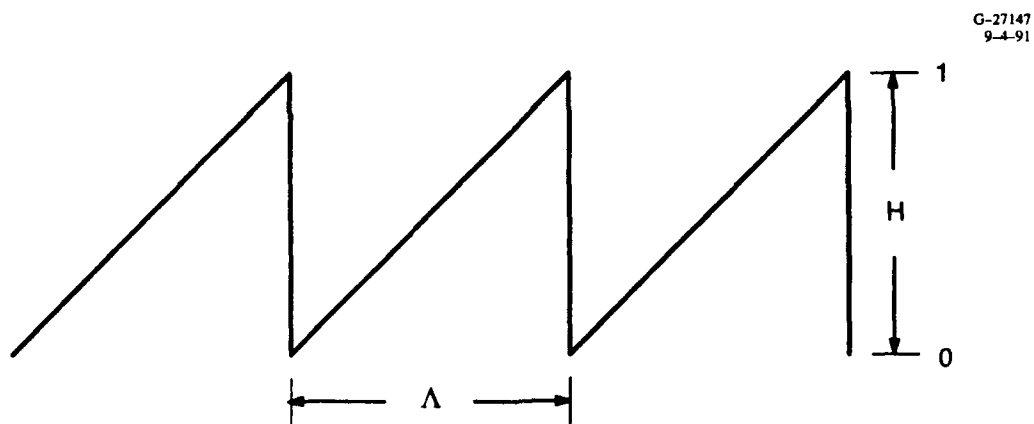


**Figure 1** Cross-Sectional View of Sawtooth Wave (From Ref. 1)

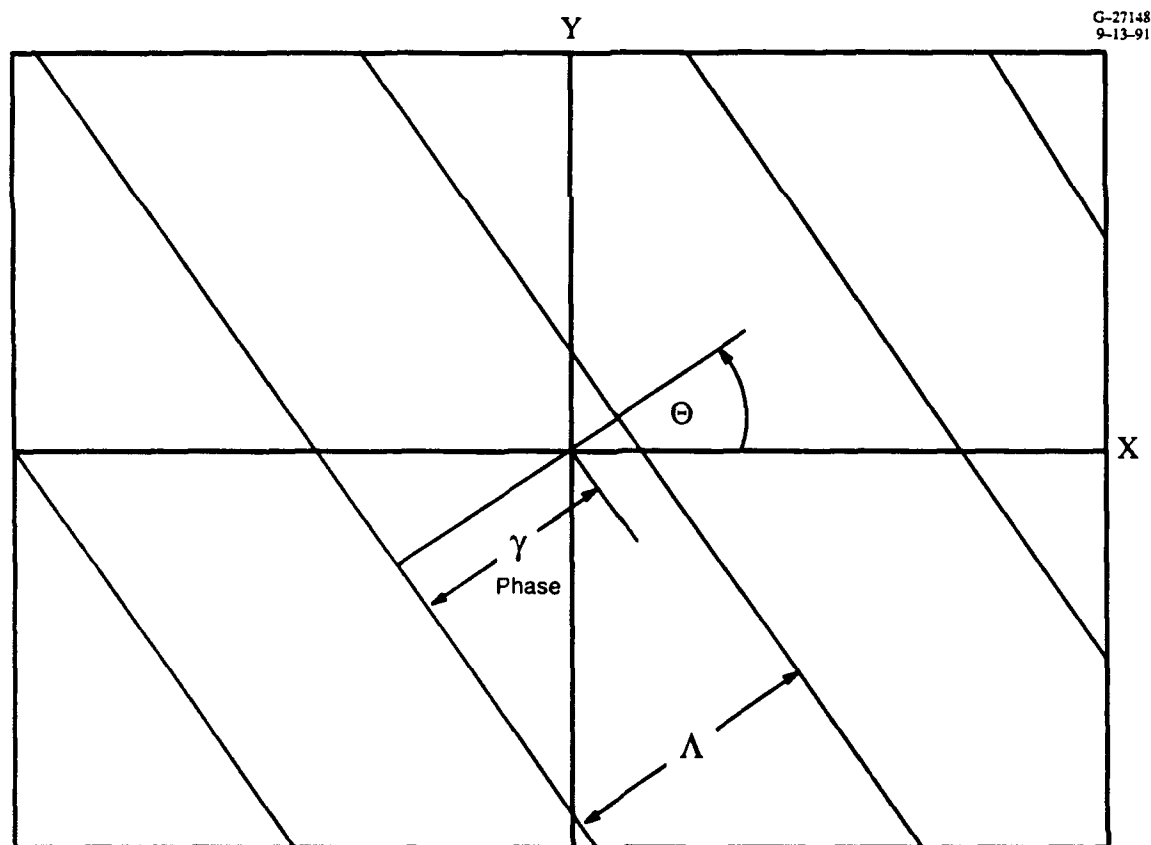


**Figure 2** Formation of Sawtooth Waves in Horizontal Domain (From Ref. 1)

At each grid point the  $N$  individual wave heights are summed. For large  $N$ , the Central Limit Theorem can be applied, and a normal deviate (ND) for each gridpoint is calculated as follows:

$$ND(x,y) = \sqrt{\frac{12}{N}} \left[ \sum_{n=1}^N H_n(x,y) - \frac{N}{2} \right] \quad (2.2-1)$$

where

- $N$  is the number of waves
- $H_n$  is the height of a single wave at point  $(x,y)$
- $x,y$  are the coordinates of a grid point on the horizontal plane.

Once the two-dimensional perturbation field has been generated, a candidate threshold value (dependent on the fractional cloud cover of the particular cloud layer) is calculated and applied to the field. Values falling above the threshold are deemed to be cloud, those below are clear. The threshold value is calculated by converting the desired fractional cloud cover (cumulative probability) to a normal deviate by the following equation (Ref. 8) where  $p = 1 - \%$ cloud cover,  $a = 2.30753$ ,  $b = 0.27061$ ,  $c = 0.99229$  and  $d = 0.04481$ :

$$\begin{array}{ll} \frac{p > 0.5}{k = 1} & \frac{p \leq 0.5}{k = -1} \\ t = \sqrt{\ln[1/(1 - p)^2]} & t = \sqrt{\ln[1/p^2]} \end{array}$$

$$THRESH = k * [t - (a + bt)/(1 + ct + dt^2)]. \quad (2.2-2)$$

The candidate threshold may be slightly off due to two factors: we use a discrete (though relatively large) number of waves to create the field, and we sample the field at a limited number of grid points. This results in small deviations from the specified cloud/clear amounts after applying the recommended threshold. For the prototype model, an iterative process was developed to slightly vary the threshold until the correct fractional coverage was produced. When simulating cloud climatology (one of the main uses of the BSW model), slight deviations from the exact fractional coverage in any one cloud scene from a number of realizations may be acceptable. Greater accuracy (and thus the iterative threshold process) is required when modeling individual cloud scenes.

The structure of the stochastic fields generated with the BSW model depends on two model parameters; the number of waves and the wavelength(s) (more than one wavelength may be used in any one scene). Sequences of two-dimensional cloud scenes produced with varying numbers of waves and wavelengths are shown in Figs. 3 and 4. Each of the scenes in the two figures has horizontal dimensions of 50 km by 50 km, and all are binary cloud/no cloud scenes with 50% cloud cover.

The six scenes shown in Fig. 3 were all generated with two different wavelengths; half of the total number of waves had  $\lambda = 40$  and the remainder had  $\lambda = 55$  km. By comparing the cloud fields generated with smaller and larger number of waves, it is clear that a large number of waves (approximately 200) is required to produce realistic cloud fields with these wavelengths. This is unlike the application of the BSW algorithm to cloud climatology where a small number of waves ( $N = 12$ ) may be sufficient (Ref. 1), and climatology is based on a large number of realizations. Unfortunately, due to the large number of waves required to generate any single cloud scene, the initial attraction of low computational cost offered with the BSW model becomes less compelling.

Figure 4 shows a sequence of cloud scenes with wavelengths ranging from 10 km to 200 km (all generated with 200 waves). The wavelength is a measure of the "scale distance" of the clouds in the scene. Scale distance (as defined in Ref. 1) is the distance over which the spatial correlation coefficient remains at or above 0.99. The wavelength is directly proportional to the scale distance as

$$\lambda = c * r \quad (2.2-3)$$

where  $\lambda$  is wavelength (km),  $r$  is scale distance (km) and  $c$  is a multiplicative constant. The constant  $c$  was taken to be 340 in Ref. 1 (for 2-d clouds) and 256 in Ref. 2 (for 3-d clouds), corresponding to wavelengths of 340 and 256 km, respectively, with a correlation distance of 1 km. We found (see Fig. 4) that using wavelengths of that scale resulted in cloud scenes with a large number of triangular artifacts. To generate natural-looking individual scenes, it was necessary to use smaller wavelengths in the BSW algorithm. We can use the qualitative definition of scale distance to produce cloud fields representative of different cloud types.

Because stratocumulus clouds tend to group into smaller masses than stratus clouds, we expect that the scale distance for Sc is lower than that for St clouds. Accordingly,



5 Waves



20 Waves



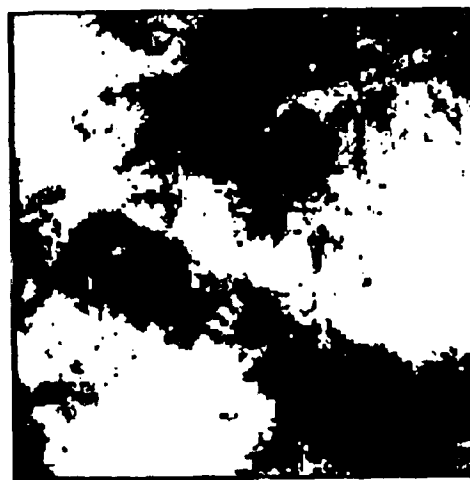
50 Waves



100 Waves

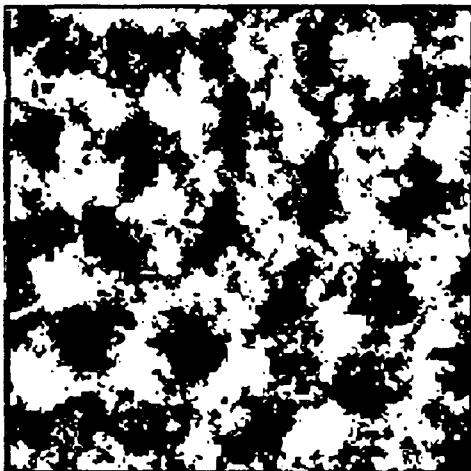


200 Waves

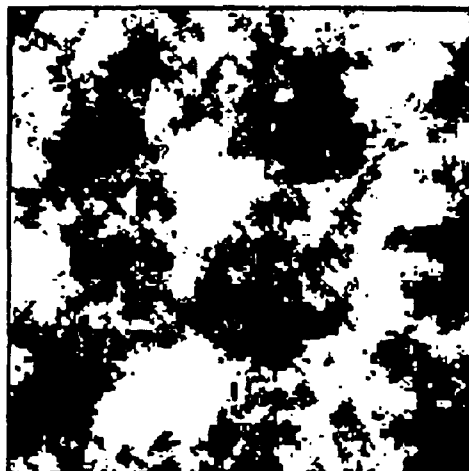


300 Waves

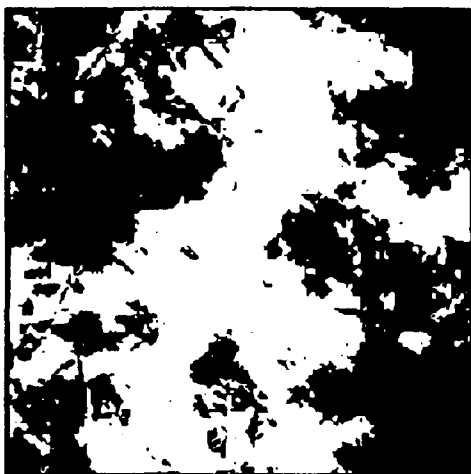
**Figure 3** Sequence of Binary Cloud Scenes (50% Cloud Cover,  $50 \times 50$  km Horizontal Domain) Generated with the Two-Dimensional BSW Method with Differing Number of Waves



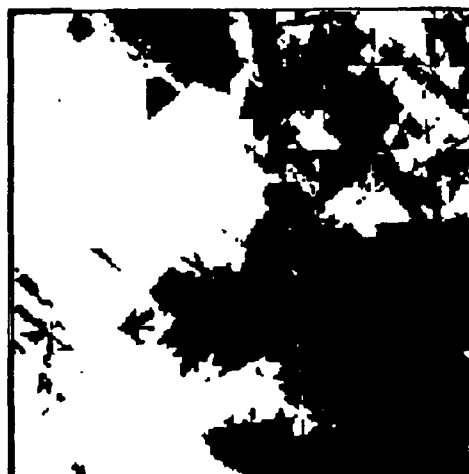
$\lambda = 10$



$\lambda = 20$



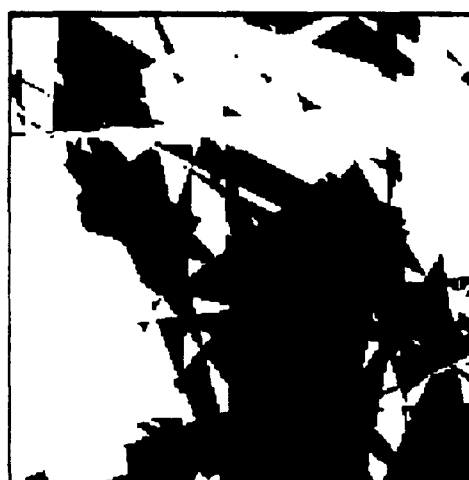
$\lambda = 40$



$\lambda = 80$



$\lambda = 120$



$\lambda = 200$

**Figure 4** Sequence of Binary Cloud Scenes (50% Cloud Cover,  $50 \times 50$  km Horizontal Domain) Generated with the Two-Dimensional BSW Method with Various Values for the Wavelength (in km)

we use smaller wavelengths in the BSW model to produce cloud scenes representative of stratocumulus, and larger wavelengths for stratus cloud type. In the prototype model we define a set of two wavelengths for each cloud type: 40 and 55 km for Sc and Ac, 110 and 130 km for St and As. These values were chosen because they result in qualitatively realistic cloud distributions within each realization. With this in mind, these values are not directly related to the scale distance (defined in terms of correlation distance) discussed in Ref. 1.

*Generate Upper Cloud Surface* — Based on visual analysis of various cloud types we chose to approximate the vertical structure of stratiform clouds (the only types considered in the prototype model) by a coarse dome with higher resolution random variations superimposed upon it. It was clear that for this approximation, variations based on simple “white noise” would not be realistic. Instead, random variations along the dome-like structure could be generated with algorithms approximating fractional Brownian motion. FBM models are a subset of an even broader group of random fractal models. We begin this section with a brief overview of fractals and then later describe the application of this technique to the generation of the upper cloud surface of stratiform clouds within the cloud model.

The most common of the random fractals is ordinary Brownian motion (commonly known as the random walk model). In one dimension, Brownian motion can be modeled by sampling a random variable,  $V$ , over a real variable  $t$  (time). The function  $V(t)$  represents the displacement of a particle (as measured from the origin) undergoing Brownian motion. Increments in  $V(t)$  are Gaussian distributed with variance proportional to the time difference as follows (Ref. 9):

$$\text{Var}( V(t_2) - V(t_1) ) \propto | t_2 - t_1 | . \quad (2.2-4)$$

Such increments are independent and statistically self-similar. That is, if we were to expand or contract the one-dimensional function,  $V(t)$ , in the time dimension we would generate a statistically indistinguishable function with increments scaled appropriately,

$$V(t_0 + t) - V(t_0) \text{ is scaled to } \frac{1}{\sqrt{r}} (V(t_0 + rt) - V(t_0)) \quad (2.2-5)$$

where  $r > 0$ . An example of the scaling properties of Brownian motion is shown in Fig. 5.



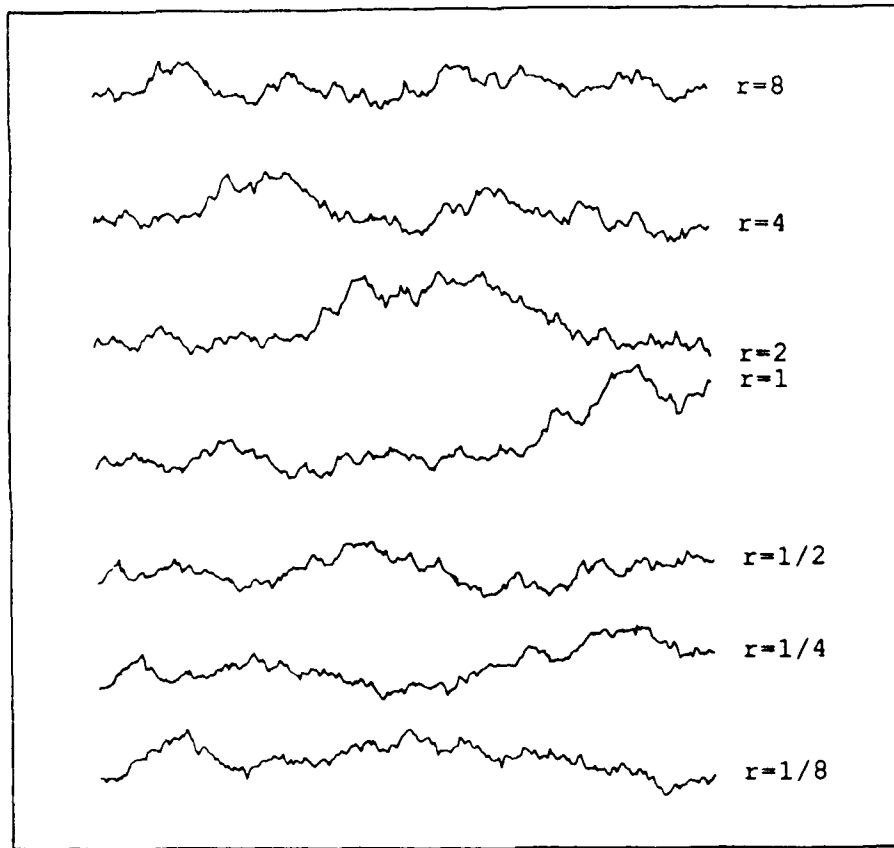


**Figure 5** Brownian Motion With Scale Factors Ranging from  $r=1/8$  to  $r=8$  Corresponding to Expanding and Contracting the Original Function Along the Horizontal Direction (From Ref. 3)

Fractional Brownian motion is a generalization of Brownian motion in which Eq. 2.2-4 is modified to

$$\text{Var}( V(t_2) - V(t_1) ) \propto | t_2 - t_1 |^{(2H)} \quad (2.2-6)$$

where  $H$ , the Hurst parameter, can vary between 0 and 1. Unlike Brownian motion (i.e.,  $H = 0.5$ ), increments of FBM are not independent, but are positively ( $H > 0.5$ ) or negatively ( $H < 0.5$ ) correlated. As a result, FBM can be used to model random fields representative of highly correlated stratus clouds or somewhat less correlated stratocumulus clouds in two, three or four dimensions. Figure 6 shows one-dimensional fractional Brownian motion with various values for the Hurst parameters.

One elementary method for approximating fractional Brownian motion is the mid-point displacement method. In this method, FBM is generated over a specified interval (e.g.,  $0 < t < 1$ ) by a recursive interpolation algorithm. The value of the function at time

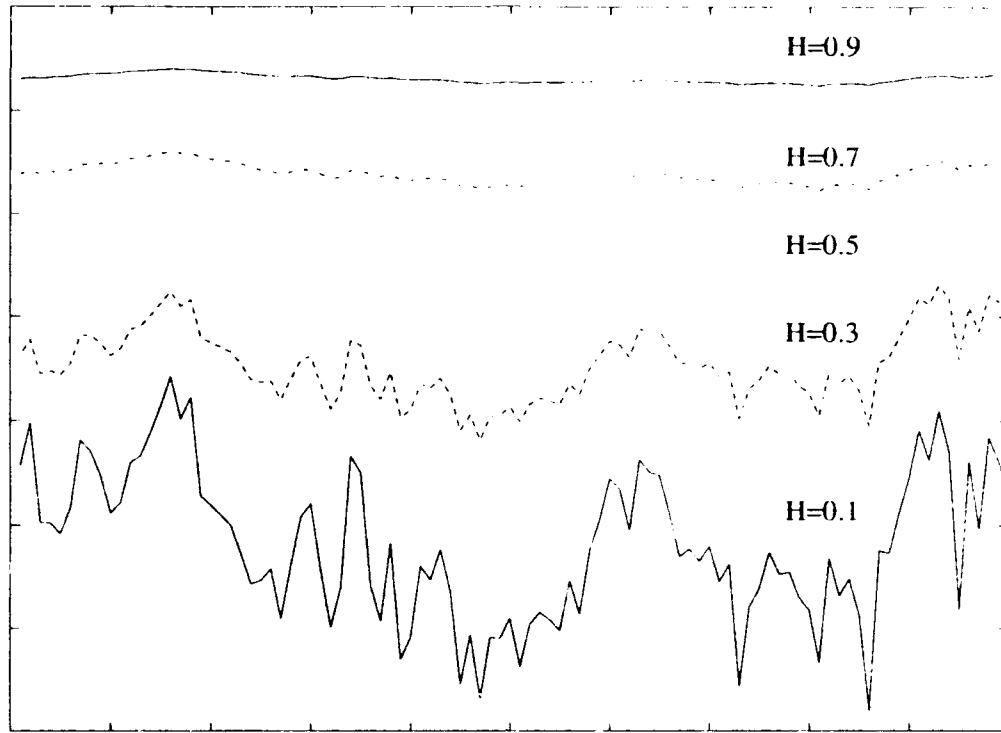


**Figure 6** Fractional Brownian Motion With Various Values of the Hurst Parameter, Lacunarity Parameter = 0.5

zero,  $V(0)$ , is set to zero and  $V(1)$  is sampled from a Gaussian distribution with variance  $\sigma^2$ . The first step consists of calculating  $V(1/2)$  as the average of  $V(0)$  and  $V(1)$  and then adding a Gaussian random offset with variance  $\Delta_1^2$  to that averaged value. In successive steps, we continue to calculate consecutive midpoints, adding random offsets with corresponding variance for each. Figure 7 shows the function  $V(t)$  after two steps of the midpoint displacement algorithm. Midpoint random offsets are indicated by the vertical line segments. It can be shown (Ref. 3) that at step  $n$  the variance of the random offset is

$$\Delta_n^2 = \frac{\sigma^2}{(2^n)^{2H}} (1 - 2^{2H-2}). \quad (2.2-7)$$

At each step, the resolution is increased by a factor of 2 with the number of points increasing as  $2^n+1$ . Using this method, visible artifacts of the first few steps in the recursion are frequently visible in the final function. The Successive Random Additions (SRA) method is an extension of the midpoint displacement method developed to avoid these artifacts. In this method random offsets of suitable variance are added to all of the points at each

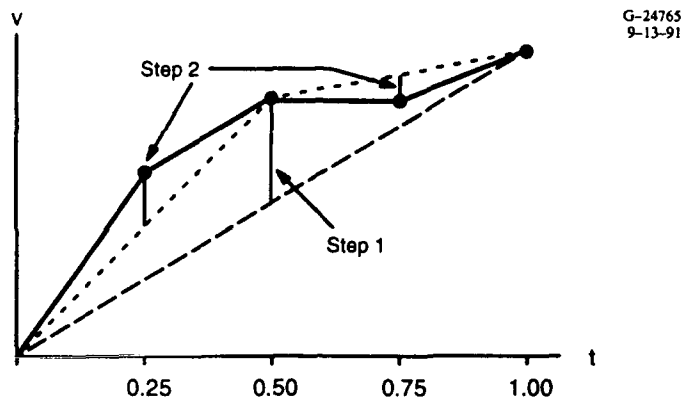


**Figure 7** Two Steps of the Midpoint Displacement Method

step in the recursion, not just at the midpoints (resulting in slightly higher computational costs than the standard midpoint displacement technique).

A further extension to the SRA method provides the user with more flexibility in the generation of the final function. The extension allows for interpolation to points other than the midpoint, thus increasing the resolution by factors other than 2 at each stage. The parameter that controls the rate of interpolation in the algorithm is the lacunarity parameter,  $r$ . Varying  $r$  changes the total number of steps required to generate the fractional Brownian motion and thus the amount of variability in the final function. The variance of the random offsets in the SRA method takes on a slightly more complicated form than in the midpoint displacement algorithm, but also depends on the value of  $n$ . The variance can be written as

$$\Delta_n^2 = \frac{\sigma^2}{2} (1 - r^{2-2H}) (r^n)^{2H}. \quad (2.2-8)$$

A sequence of time series generated with various  $r$  values ( $0 < r < 1$ ) is shown in Fig. 8.

In the prototype cloud model, we use the one-dimensional SRA method to generate random structure along line segments forming the coarse backbone of the upper cloud surface. The coarse backbone is first generated by traversing the two-dimensional cloud/no cloud field generated with the BSW, identifying continuous lines of cloud elements (the field is traversed in both the  $x$  and  $y$  directions independently). Each continuous line of cloud elements is divided into four smaller segments and the coarse structure built upon those segments as shown in Fig. 9.

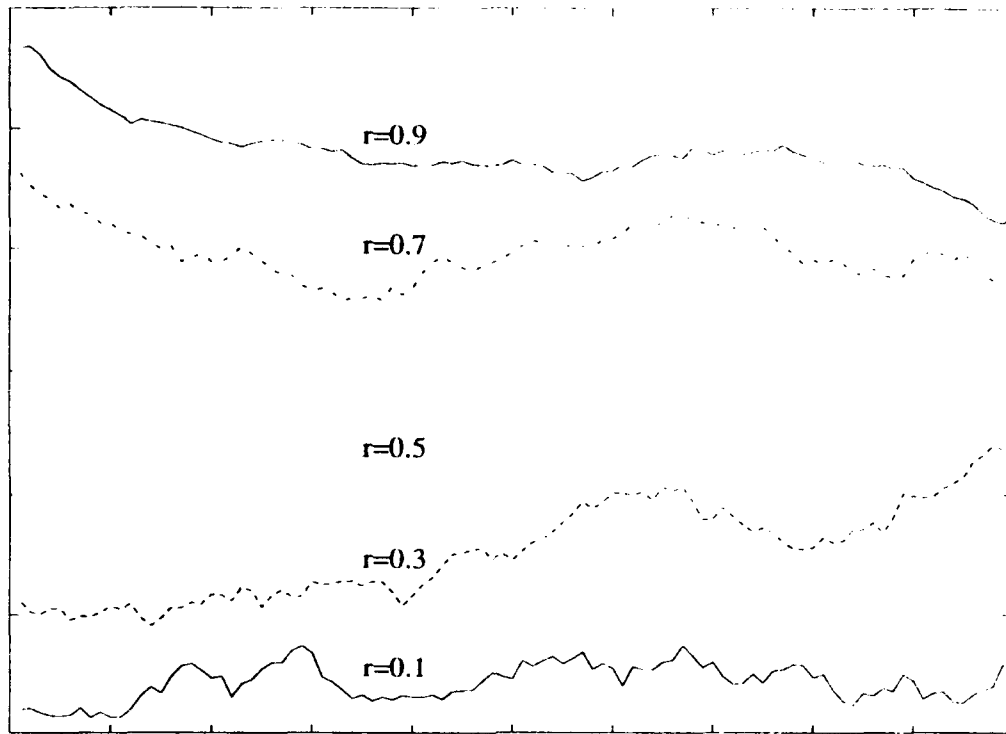


**Figure 8** Fractional Brownian Motion with Various Values of the Lacunarity Parameter, Hurst Parameter = 0.7

Coarse structure is defined so that the apex of the larger clouds (i.e., those whose horizontal extent is at least 10% of the total horizontal cloud domain size) reaches the user-specified cloud top height. The apex of the smaller cloud elements (those whose horizontal extent is less than 10% of the cloud domain size) extends to 50% of the specified thickness above the base. Having specified the end points of each of the four segments, the SRA method is used to generate random structure between each set of adjacent end points. Height values generated in this manner are stored as  $HGT_x(x,y)$  and  $HGT_y(x,y)$ , corresponding to traversing the cloud field in the x and y directions, respectively. A smoothed upper cloud surface is defined by averaging the two heights at each x-y gridpoint as

$$HGT_{\text{smoothed}}(x,y) = \frac{1}{2} (HGT_x(x,y) + HGT_y(x,y)). \quad (2.2-9)$$

This technique produces upper cloud surfaces that overall are quite realistic, but which sometimes result in edge artifacts as discussed in Section 2.2.3 and shown in Fig. 13. In that figure, sharp drop-offs can be seen near some areas of the cloud edge. Because of these artifacts, we have replaced the method outlined here with an alternate technique in the interim model.

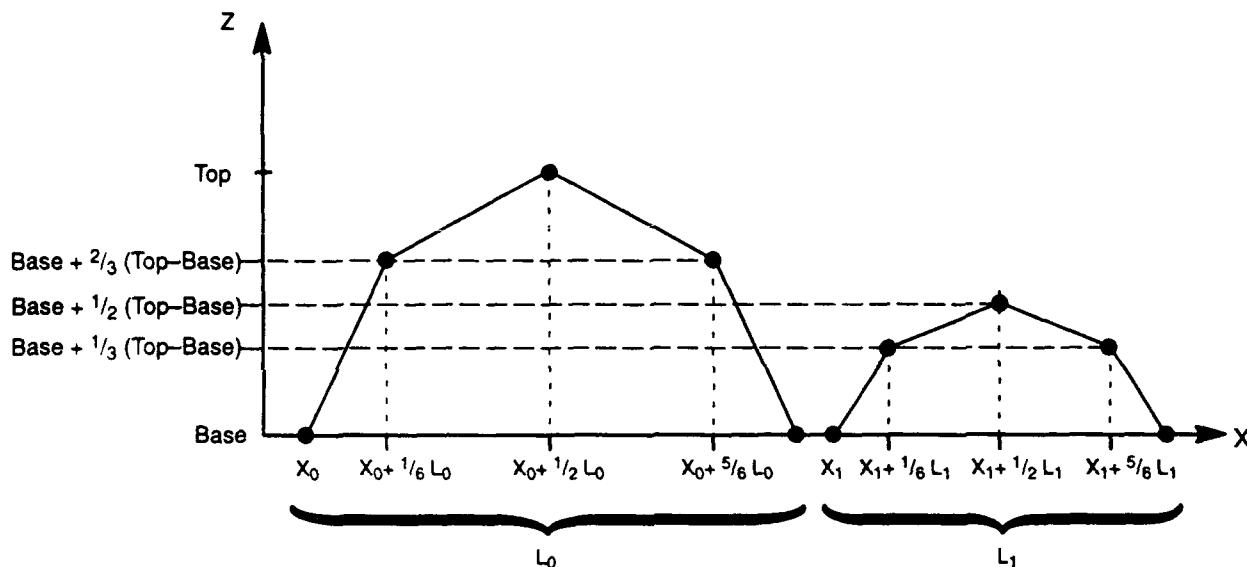


**Figure 9** Fundamental Structure Used in Dome-Building Process to Generate Upper Cloud Surface

*Generate Lower Cloud Surface* — We use a two-dimensional version of the SRA model described in the previous section to generate the relatively smooth yet variable cloud base surfaces characteristic of stratiform clouds. The lower cloud surface is defined as a 2-d perturbation field. The SRA algorithm is used to generate the perturbation field which is then scaled to have mean equal to the user-specified cloud base and a standard deviation of 10% of the cloud layer thickness. In the absence of quantitative data of the variance of typical cloud base surfaces, a value of 10% is assumed because it results in visually realistic lower cloud surfaces.

In two dimensions we initialize the SRA algorithm at each of the four outer corners of a two-dimensional square grid. Initially all four corners are set to zero. We then interpolate recursively (using bilinear interpolation) to compute the nominal value of the function at each grid point. At each step the value of the function at each "new" point,  $V_{\text{new}}(x,y)$ , is the weighted average of the four nearest "old" points (i.e., those grid points computed during the previous step in the recursion). Weighting is based on the relative distance from the

new point to each of the old points as shown in Fig. 10. The distance values,  $dx$  and  $dy$  vary between zero and one, and are used in the interpolation as follows:

$$\begin{aligned}
 V_{\text{new}}(x,y) = & (1-dx) * (1-dy) * V_{\text{old}}(x_0,y_0) + \\
 & (1-dx) * dy * V_{\text{old}}(x_0,y_1) + \\
 & dx * (1-dy) * V_{\text{old}}(x_1,y_0) + \\
 & dx * dy * V_{\text{old}}(x_1,y_1).
 \end{aligned}
 \tag{2.2-10}$$

Random offsets are then added to  $V_{\text{new}}$  at all grid points before proceeding to the next step in the recursion. Here, as in 1-d, we can tailor the structure of the cloud base surface by carefully selecting Hurst and lacunarity parameter values. Default values for  $H$  and  $r$  in the prototype cloud base model are 0.8 and 0.5, respectively, for all cloud types.

*Generate Internal Cloud Structure* — Within the schedule of the Cloud Scene Simulation Project, Task 2 (development of the prototype model) occurred much before the analyses and studies scheduled as Task 3. Therefore, in the absence of any detailed analysis of the internal liquid water structure of stratiform clouds, we decided to build the internal structure of the cloud scene based on a three-dimensional stochastic field generation technique for the reasons outlined in Table 1. To facilitate comparison, we implemented three-dimensional versions of both the BSW and SRA models described previously.

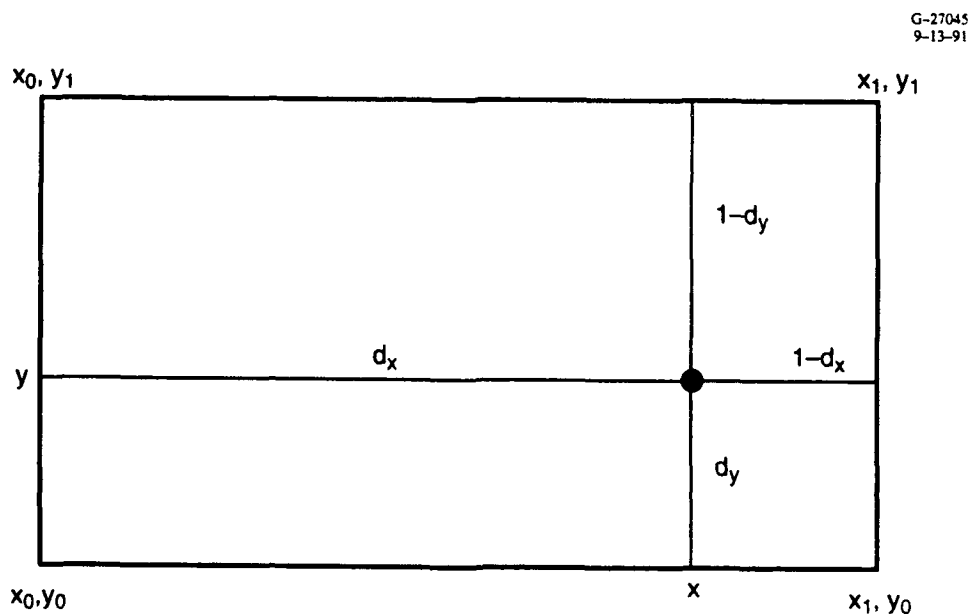


**Figure 10** Variables Used in Bilinear Interpolation (See Eq. 2.2-10)

Comparison of the internal liquid water content (LWC) fields resulting from both of these models with aircraft measurements is an important aspect of Task 3 — Studies and Analyses.

The extension of the BSW algorithm to three dimensions is described in Ref. 2. N waves are superimposed in the three-dimensional space bounded by the maximum cloud base and top heights. Random phase and orientation are required for each wave as before, although in three dimensions, three angles ( $\alpha, \beta, \gamma$ ) are used to describe the orientation of each wave with respect to the origin. Figure 11 shows a sawtooth wave in three-dimensions where the wave is oriented such that all points on the plane ABC have the same wave height. The angles ( $\alpha, \beta$  and  $\gamma$ ) are the angles that the shortest line between the origin (O) and the plane ABC make with the x, y and z axes, respectively. As before, it was found that a large number of waves (100 were used in the model) was needed to avoid the presence of triangular artifacts in the final field. As discussed in Ref. 2, we scale the vertical coordinate used in the BSW model to retain the correct spatial variations between the horizontal and vertical coordinates. The vertical coordinate is scaled by the ratio of the horizontal cloud domain extent to the cloud layer thickness.

The extension of the SRA model to three dimensions is straightforward. We initialize the function at the eight outer corners of a cube and proceed to interpolate in three dimensions such that  $V_{\text{new}}(x,y,z)$  depends on the value of the function  $V_{\text{old}}$  at each of eight surrounding points. Random offsets are then added to each point as before. By varying the Hurst and lacunarity parameters, (controlling the interpolation rate and overall amount of variance in the scene) scenes of varying statistical character can be produced. Again, we effectively scale the vertical coordinate used in the model by using a different lacunarity parameter in the vertical than in the horizontal coordinate directions.

Once the 3-d perturbation field has been generated (using either the BSW or SRA model), it is converted to a field of liquid water density values. Assuming a horizontally homogeneous temperature profile, the temperature and vertical location of each level in the cloud scene is used, along with cloud type information, to specify the mean liquid water density value within the level following the method outlined by Feddes in Ref. 7. Using Feddes' method for a given cloud type and temperature, the maximum condensed moisture content (in  $\text{g/m}^3$ ) is retrieved from a look-up table. (That look-up table is reproduced here in Table 3.) Recall that only stratus, stratocumulus, altostratus and altocumulus

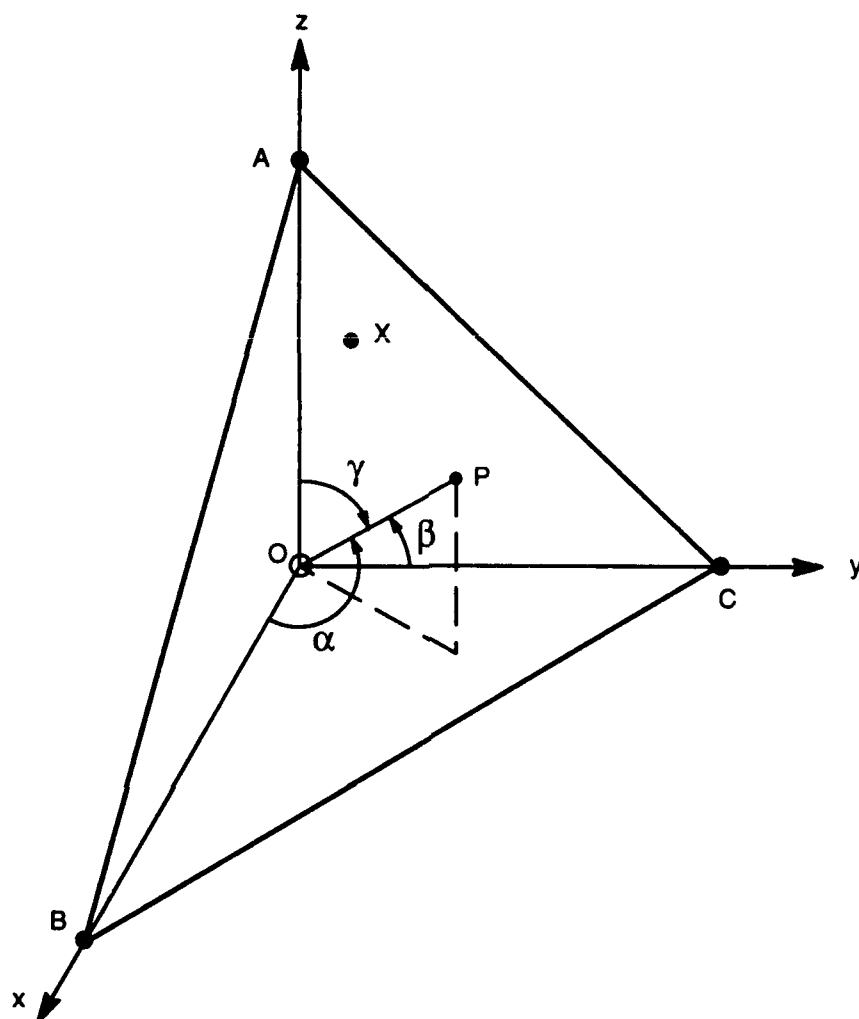


**Figure 11** Three-Dimensional Geometry Used in the BSW Method. All points on the Plane ABC have Constant Wave Height. The line OP is the Shortest Distance from the Origin to the Plane and Has Angles  $\alpha, \beta, \gamma$  with the x,y and z Axes (from Ref. 2)

cloud types are simulated in the prototype model. Other moisture values are listed here for comparison.

The actual LWC at any height  $z$  within a cloud layer is some fraction of the maximum condensed moisture based on its position above the cloud base. It can be given by the following:

$$lwc(z) = (lwc_{max}) (\% \text{ cover}) F \quad (2.2-11)$$



**Table 3      The Maximum Condensed Moisture (in g/m<sup>3</sup>) that can Occur in a Nonprecipitating Cloud as a Function of Cloud Type and Temperature (from Ref. 7). Cloud Types simulated in the Prototype Model are Highlighted**

CLOUD TYPE	TEMPERATURE (DEGREES C)									
	<-25	-25 to -20	-20 to -15	-15 to -10	-10 to -5	-5 to 0	0 to +5	+5 to +10	+10 to +15	<+15
ST	.10	.15	.20	.25	.30	.35	.40	.45	.50	.50
SC	.20	.30	.40	.45	.50	.55	.60	.70	.70	.70
CU	3.0	3.0	3.0	3.0	3.0	3.0	3.0	3.0	3.0	3.0
NS	.35	.40	.45	.50	.60	.60	.75	.90	.90	.90
AC	.25	.30	.35	.40	.40	.45	.60	.70	.70	.70
AS	.15	.20	.25	.30	.30	.35	.40	.50	.50	.50
CS	.15	.15	.15	.20	.20	.20	.25	.25	.25	.25
CI	.10	.10	.10	.10	.15	.15	.15	.20	.20	.20
CC	.05	.05	.05	.05	.10	.10	.10	.15	.15	.15
CB	6.5	6.5	6.5	6.5	6.5	6.5	6.5	6.5	6.5	6.5

where  $lwc_{max}$  is the maximum condensed moisture (a function of cloud type and temperature), %cover is the fractional cloud cover in the layer and F is a function of percentage height of z above the cloud base. The fraction, F, is determined from empirically-derived curves shown in Ref. 7. One of those curves has been included here as Fig. 12 relating the percent height above cloud base to the fraction of maximum condensed moisture for Sc and Ac clouds. Figure 12 is concerned only with non-precipitating clouds (and thus F only reaches a maximum of approximately 75%). The equation of this curve is

$$F = 0.236 + 0.018974 (\%) - 0.00018974 (\%)^2 \quad (2.2-12)$$

where (%) is shorthand for the percent height above cloud base (0-100). As an example, let us find the mean LWC at a level 200 meters up into a 600 meter stratocumulus cloud layer (40% fractional coverage) where the temperature at that height is +8 deg C. First, we find the maximum condensed moisture value for a stratocumulus cloud at that temperature from Table 3 to be 0.7 g/m<sup>3</sup>. Then, using Fig. 12, we read off a percent of maximum

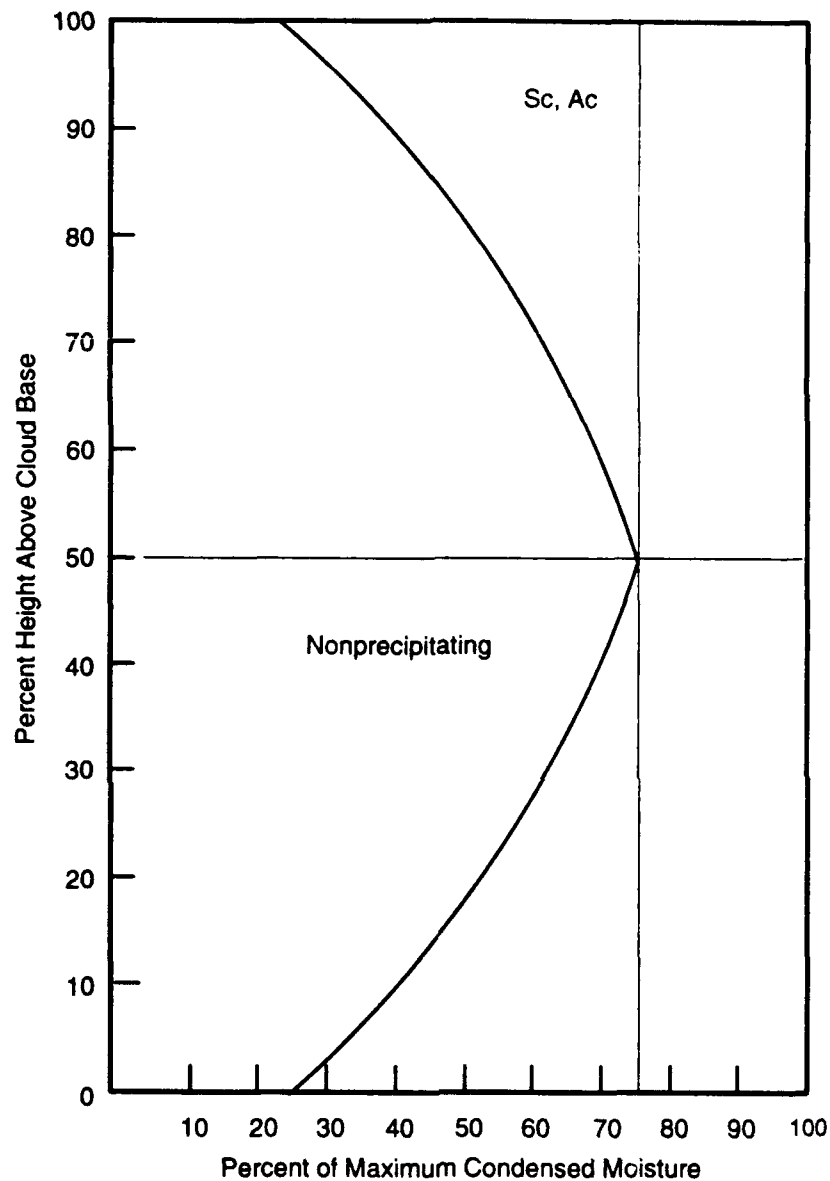


**Figure 12** Profile of Percent of Maximum Condensed Moisture for Sc and Ac Cloud Types Used in the Computation of Mean LWC for a Given Level in a Cloud Layer (From Ref. 7)

condensed moisture of 65%, corresponding to a percent height above the base of 33%. The final mean value of the layer is then

$$l_{wc} = (0.70)(0.4)(0.65) = 0.182 \text{ g/m}^3. \quad (2.2-13)$$

At each vertical level in the 3-d cloud field we transform the zero-mean Gaussian field to have mean LWC (computed as above) and coefficient of variation of 10% (where the coefficient of variation is a measure of variation with respect to the mean). Choosing the coefficient of variation equal to 10% was convenient and reasonable for the prototype model. Later modifications to the cloud model will provide a distributional form consistent with results from an analysis of cloud data.

Finally, as a means to introduce variability near the cloud edges, we set those field values near the edge that are below a certain value ( $V(x,y) < \bar{V}(1-c)$ ) equal to zero (where  $\bar{V}$  and  $c$  are the mean and coefficient of variation of the 3-d cloud field, respectively). This results in more realistic cloud scenes with holes and disconnected cloud elements near the edges as found in nature.

*Write Three-dimensional Cloud Field to Output File* — The output module writes the three-dimensional array of liquid water content values to an output file. Each of the two possible cloud layers in the prototype model are written to separate files (with “.L” and “.M” appended to the filename for low and middle layers, respectively). This output module is called by the main interface routine and is designed to be replaceable if the user requires a different format to store the cloud data.

A header record is generated at the start of each of the output files. This header contains the size and resolution of the cloud domain and the height of the lowest cloud element. This information about layer position and scale can be used as input for further processing of the cloud field. See Ref. 6 for further details about the content and format of the output files.

### **2.2.3 Results and Conclusions**

The prototype model was developed rapidly to demonstrate a capability to produce realistic three-dimensional cloud fields. Because the Studies and Analyses task occurs later in the project, we did not emphasize the generation of fields with the correct spatial distribution of liquid water at this early stage. Instead we produced clouds with realistic appearance and set up the machinery to generate liquid water content structure. Comparative evaluation of the various stochastic field generation techniques will be an important task later in the project.

Figures 13 and 14 show cloud scenes produced with the prototype model. In the first figure we have a rather realistic 50% stratus layer scene. The second figure contains a less realistic realization of the same scene, generated with identical input parameters with exception of the random number seed. These two figures show both the success of the rapid prototype model and the need for improvement.

Areas in need of improvement include the generation of the horizontal cloud field and the upper bounding cloud surface. We found, based on a large number of scene simulations, that even with a large number of waves and two wavelengths, triangular artifacts resulting from the "sawtooth" nature of the BSW algorithm were frequently apparent. To avoid these artifacts, other random stochastic field generation techniques were investigated for use in future versions of the cloud model and will be discussed later in the report.

Also apparent in Fig. 14 are steep vertical cloud edges resulting from the "dome-building" process used to create the upper cloud surface. Although the dome-shaped structure may be an acceptable approximation for some stratiform cloud types in a prototype

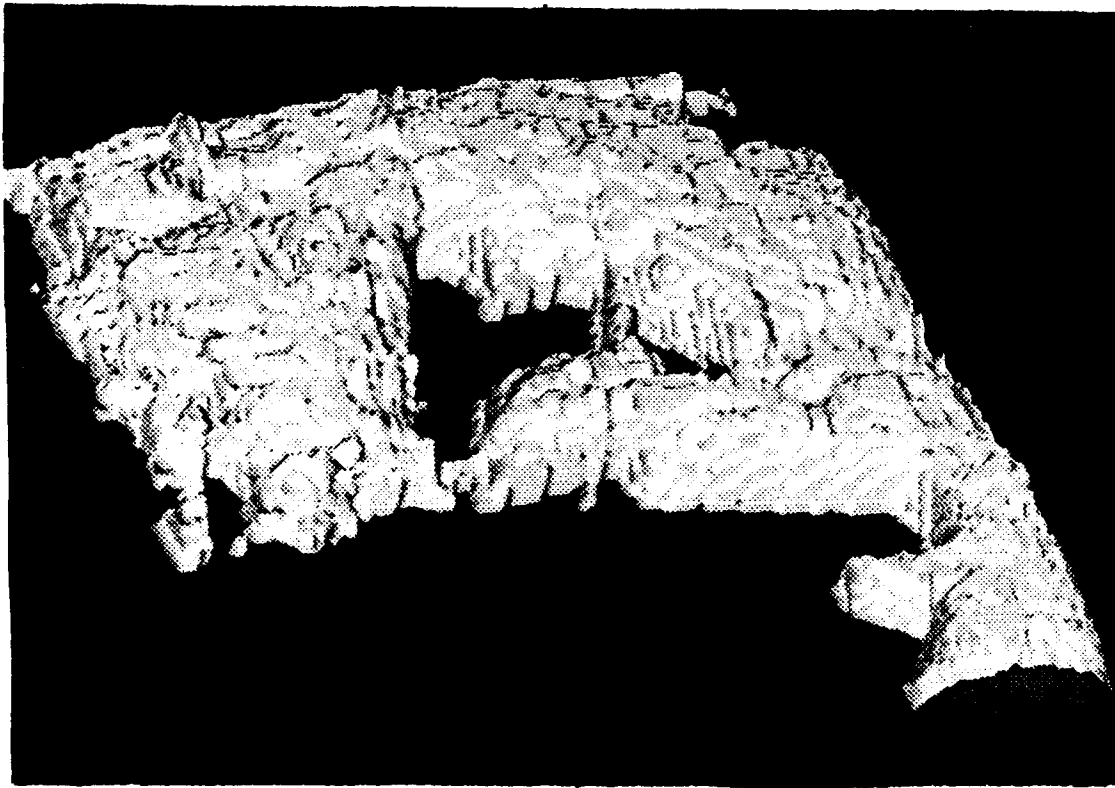


**Figure 13** 50% Stratus Cloud Layer Generated With the Prototype Model  
(20 × 20 km Horizontal Domain)

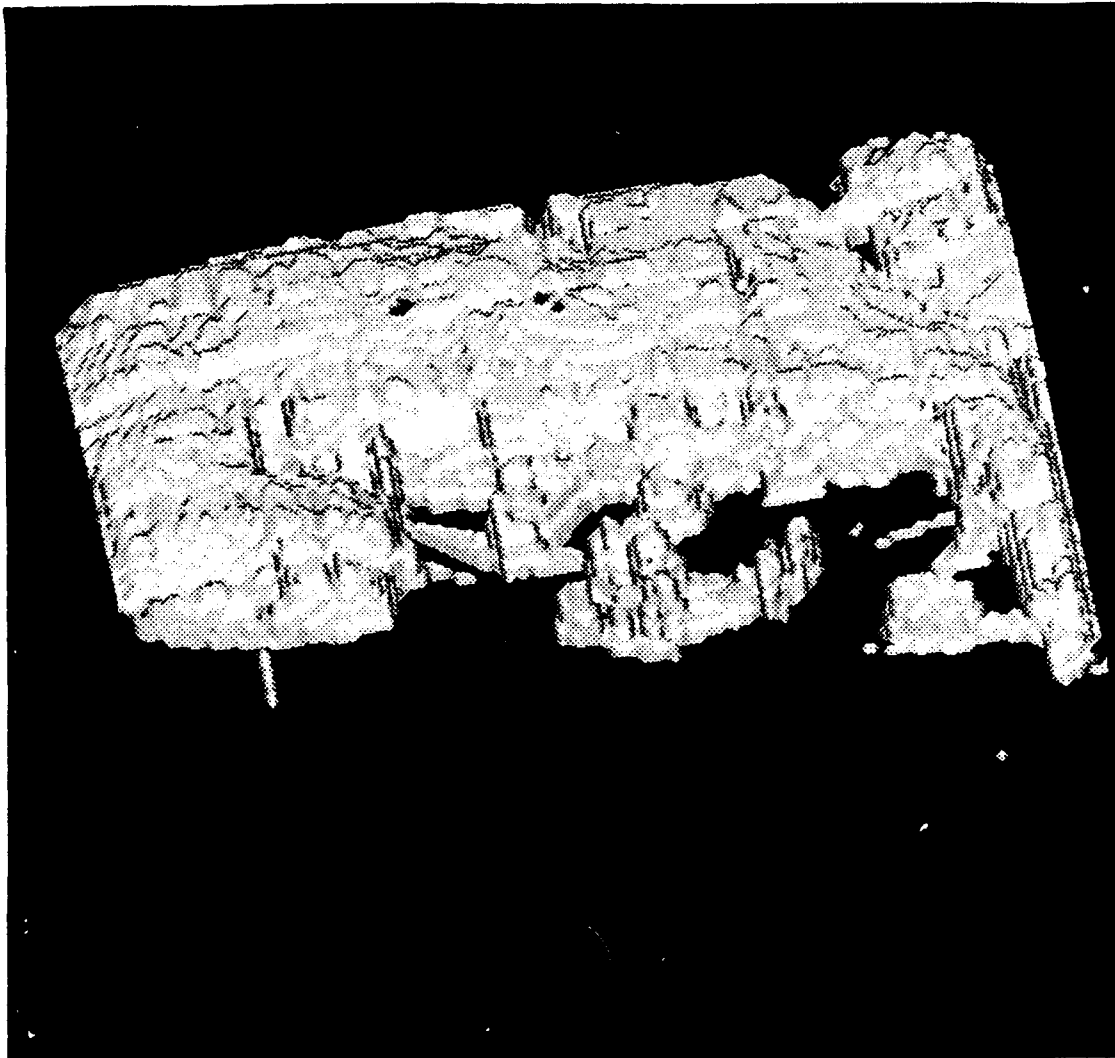


**Figure 14** 50% Stratus Cloud Layer Generated With the Prototype Model (20 × 20 km Horizontal Domain). Artifacts From the BSW Model are Clearly Visible

model, it does not represent the natural variability in cloud edges and is too inflexible to use for other cloud types. In version 2.0 we implemented a different method to build vertical cloud structure.

Additional results from the prototype model include the need to modify the memory allocation within the software to allow the user more flexibility in specifying the size, shape and resolution of the cloud domain, as well as a need to fine-tune the parameters used within the model (specifically the wavelengths used in the BSW algorithm and the Hurst and lacunarity parameters in the SRA algorithm). All of the results and ideas generated during this task were considered during the requirements analysis phase of Task 4 — Develop Model Version 2.0.

## **2.3 THE INTERIM MODEL (VERSION 2.0)**

The interim model (see Ref. 10) is built upon the tools and software developed for the prototype model. It incorporates various improvements to the previous model as well as added capabilities. Improvements in the generation of the horizontal distribution of clouds and vertical structure (as discussed in Section 2.2.3) are included. Added capabilities include a prototype cirriform model, a cloud shadow model and a unique cloud data visualization technique to support scene visualization at the Engineer Topographic Laboratories (ETL). Each of these modifications and additions are covered in greater detail in following sections. We begin, however, with a discussion of requirements analysis for Task 4.

### **2.3.1 Interim Model Requirements and Design**

As in Tables 1 and 2 we present (in Table 4) the requirements applicable to the interim model and the corresponding model design decisions made to satisfy each requirement. A few of the requirements considered for the interim model carry over from the prototype model. For example, we continue to model only the spatial component of the cloud scene (not its temporal development). We also continue to emphasize portability and maintainability in the interim model. All code is written in standard FORTRAN 77 and no external databases of meteorological information are required. By keeping strictly to these ideas we hope to minimize any future difficulties integrating with other SWOE models.

Keeping in mind the goal of developing a cloud model to simulate three main cloud types, stratiform, cirriform and cumuliform, we began with stratiform in the prototype model. We add a prototype cirriform capability in the interim model. In the final version of the model, we will develop a model for cumuliform development.

The fourth and fifth requirements listed in Table 4 refer to the development of additional capabilities external to the cloud model itself. One early use of the cloud model, for surface energy budget studies, required cloud shadow locations. We designed software to compute the location of shadows (in a user-specified ground domain) cast by a given three-dimensional cloud scene. This cloud shadow package is distinct from the cloud model software in keeping with the modular, low-maintenance emphasis in the program.

To aid and participate in SWOE simulation demonstrations at ETL, we designed visualization software to convert cloud model output files to a form that can be used in ETL's

**Table 4      Requirements and Design for Interim Model**

	INTERIM MODEL REQUIREMENTS	DESIGN DECISIONS
1	Continue rapid development in order to incorporate SWOE user feedback.	Simulate cloud scenes in three dimensions only. Do not model temporal dimension.
2	Continue to work toward 100% compatibility with other SWOE team members.	Continue to write software in standard FORTRAN 77. Make software stand-alone (i.e., require no external databases, etc.)
3	Continue to expand model capabilities.	Add prototype cirriform model and thus capability to produce three layer scenes.
4	Provide capability to generate ground shadow map of any cloud scene.	Develop shadow post-processor.
5	Deliver cloud scenes to ETL for use in scene visualization.	Develop visualization tools to generate colored polygonal cloud surfaces.
6	Increase model efficiency.	Optimize code (e.g., the process of computing a cloud cover threshold).
7	Provide user with greater flexibility in cloud layer size and resolution.	Improve memory management. Allow user to simulate a rectangular cloud domain with different resolution in each direction.
8	Improve realism of horizontal distribution of cloud elements.	Replace BSW algorithm with a fractal technique (SRA).
9	Improve cloud edges and overall shape of upper cloud surface.	Replace "dome-building" method with polynomial function of fractal field.
10	Provide easier output file management.	Concatenate all layers into one output file.

scene generation system. Through close contact with ETL a set of requirements was established. The ETL scene generation system uses a standard graphics technique of approximating a natural or computer-generated surface with a large number of colored polygonal surfaces. We chose to combine the Marching Cubes isosurface algorithm (discussed in Section 2.5) with variable coloration based on cloud density and orientation for added realism. Output from the visualization software is used at TASC (on a Stardent computer) as well as at ETL.

The last five requirements in Table 4 concern improvements to the prototype cloud model. Among them, a more flexible memory allocation module that we designed to accommodate the broader range of geometric scales (i.e., width-to-height ratios) encompassed by

cirriform and stratiform cloud types in the interim model. Also, based on experience gained with the prototype model (discussed in Section 2.2.3), changes were made to increase the visual realism of the liquid water content fields. Points 8 and 9 from Table 4 refer to those changes. Lastly, we modified the output module to concatenate all cloud layers for a single scene into a single disk file. A description of each of the major model modifications is provided in the next subsection.

### **2.3.2 Modifications Included In the Interim Model**

The interim model is composed of six major model procedures where overall processing logic is similar to that of the prototype model. The main procedures are:

- Acquire model input parameters
- Generate horizontal cloud field
- Generate upper cloud surface
- Generate lower cloud surface
- Generate internal cloud structure
- Write three-dimensional cloud field to output file.

Though every module was modified to some extent to accommodate various minor upgrades to the software between Version 1.0 and 2.0, the most important modifications were in only two modules. We present those in the following two subsections.

*Generate Horizontal Cloud Field* — Studies have shown that the horizontal structure of clouds and cloud water approximately follows fractal scaling laws over a broad range of scales (Refs. 11 and 12). Others showed that this fractal behavior varies as a function of cloud type (Ref. 13). We found, through working with the SRA fractal algorithm in the prototype model, that it is an efficient way to compute stochastic fields with a high degree of control over the structure of the final field. Therefore, we implemented (in the interim model) a two-dimensional version of the SRA model to simulate the horizontal distribution of the cloud fields.

We have discussed the 1-d SRA algorithm used to build the upper cloud surface (in the prototype model), the 2-d SRA algorithm used to generate the cloud base surface (in both model versions), and the 3-d SRA algorithm to produce internal liquid water density fields (in both versions). In this section we describe the 2-d SRA algorithm used to produce



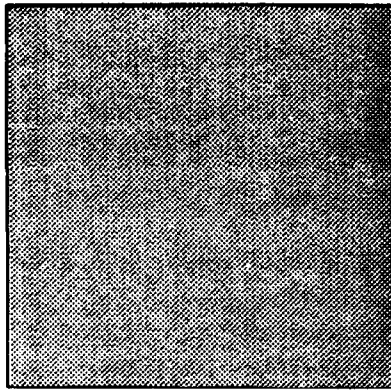
the horizontal cloud/no cloud distributions typical of distinct cloud types (e.g., cirriform and stratiform) in the interim model.

Recall the iterative process that is the basis of the SRA algorithm in 2-d. Starting with values of zero at each of four corner points, we continue to interpolate and add random offsets within the grid until the desired resolution is attained. A sequence of "snapshots" taken at consecutive steps in the generation of a two-dimensional random fractal image (256 by 256 grid points) is shown in Fig. 15. In this sequence, the intensity of the field values is represented by a grey scale, where grid points with high numerical values are lighter and darker grid points have lower values. Figure 15 shows that much of the large scale structure in the fractal field is apparent even after one step in the interpolation process. The variance of the random offsets added at each successive step decreases as in Eq. 2.2-8.

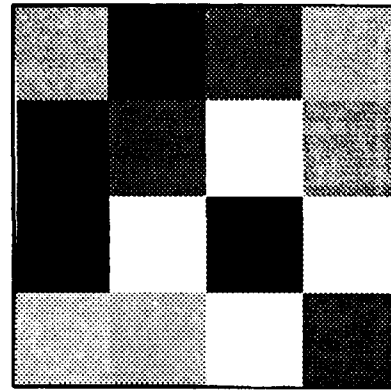
To use this gridded realization of a continuous random field to generate a binary (i.e., cloud/no cloud) scene, we select a threshold value to produce the desired coverage. In Version 2.0 of the cloud model, the threshold value is computed from a histogram of the field values. As before, all grid points with field values above the threshold are defined as "cloud," and all others are defined as "clear." Figure 16 shows a binary scene produced from the last grey-scale image displayed in Fig. 15 with the threshold chosen to yield 50% coverage.

As in the case of one-dimensional fractional Brownian motion, the visual appearance and statistical characteristics of fields generated with the SRA algorithm are highly dependent on the values of the Hurst and lacunarity parameters. We can exploit this dependency to produce fields characteristic of a variety of cloud types. Figure 17 shows the effect of varying  $H$  from 0.2 to 0.8 in four 2-d cloud scenes (with 50% cloud cover). We see that the large scale structure remains invariant for different  $H$  values. Only the smaller-scale variability (i.e., the roughness) of the field changes. We can use this property to produce fields representative of the more wispy, scattered cirrus or stratocumulus cloud types by using small  $H$  values (near 0.4). Likewise, higher values of  $H$  (near 0.7) produce more solid stratus-type cloud fields.

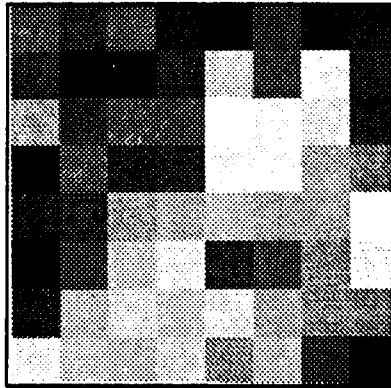
The lacunarity parameter provides another degree of freedom. Varying it effectively varies the scene texture. Lower  $r$  values ( $r < 0.5$ ) produce scenes with more, but smaller cloud elements. Higher values of  $r$  ( $r > 0.5$ ) produce scenes with fewer, but larger cloud



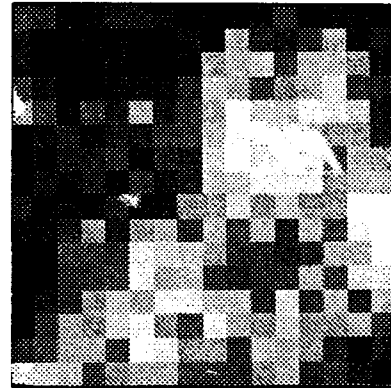
Step 1



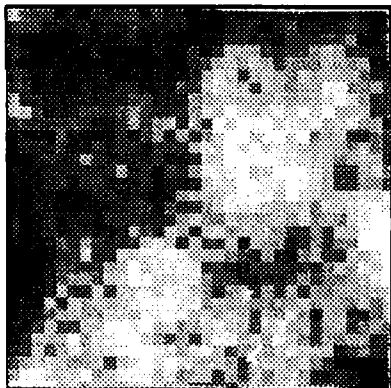
Step 2



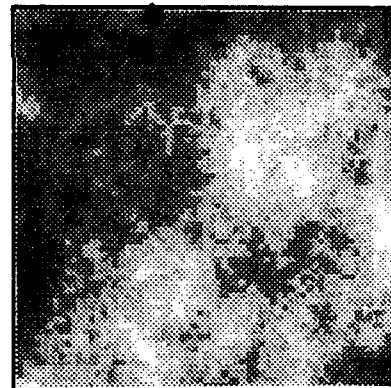
Step 3



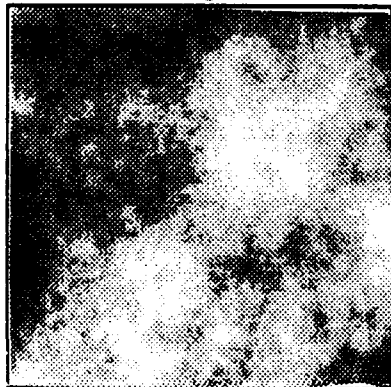
Step 4



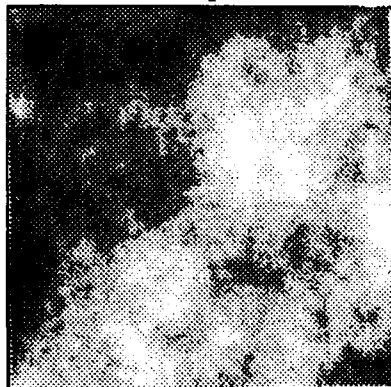
Step 5



Step 6



Step 7



Step 8

**Figure 15** Series of Images Taken at Consecutive Stages in the Development of a Two-Dimensional Cloud Field Using the Method of Successive Random Additions ( $H=0.5$ ,  $r = 0.5$ )



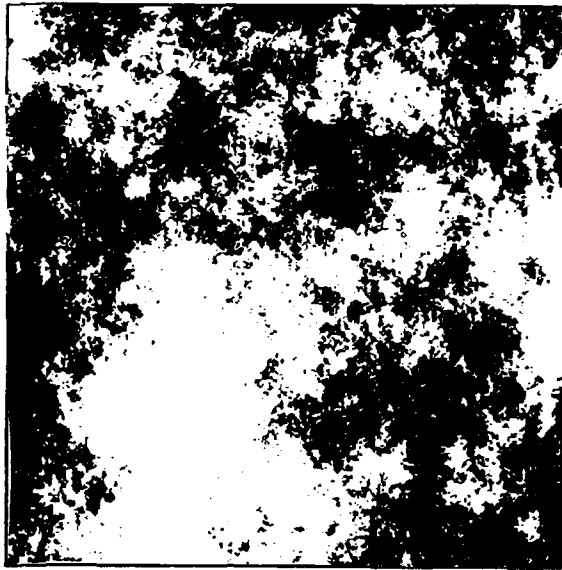
**Figure 16** Binary Cloud Field (50% Cloud Cover) Generated By Applying a Threshold Value to the Fractal Field of Fig. 15

elements. The number of points  $N(n)$  in each dimension, generated at step  $n$  in the recursion is given by

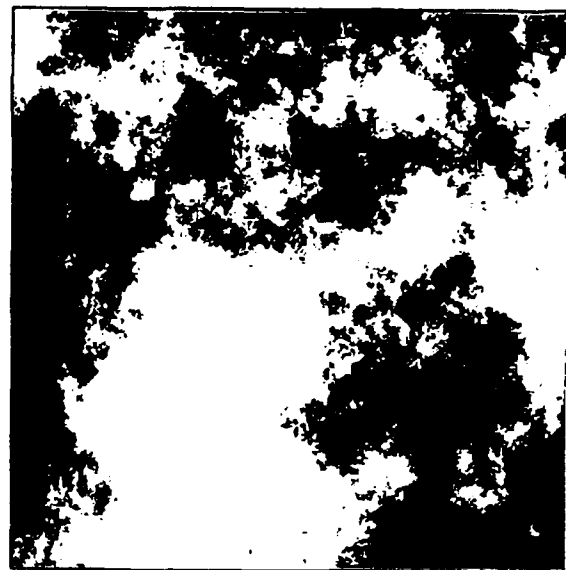
$$N(n) = \text{INT} \left[ \frac{N(n-1)}{r} \right] \quad (2.3-1)$$

where 'INTL J' represents the integer portion of the argument. From this equation one can see that lower  $r$  values generate larger numbers of gridpoints at each iteration. Consequently, fewer iterations are required to produce the desired resolution. Since the variance of the random additions decreases with each iteration, the initially large variance tends to persist more for lower values of  $r$ . In contrast, higher values of  $r$  tend to produce smoother fields using more iterations. Examples of cloud fields created with various lacunarity parameter values are shown in Fig. 18.

Given the effects that variations in the Hurst and lacunarity parameters have on the spatial characteristics of the final field, we can generate realistic images of various cloud types in two dimensions. Figure 19 provides examples of 2-d stratus, stratocumulus and cirrus cloud distributions generated using the SRA algorithm.



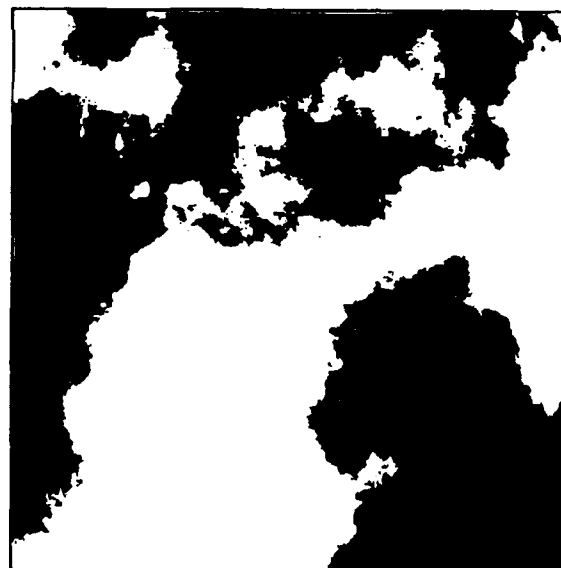
H=0.2



H=0.4

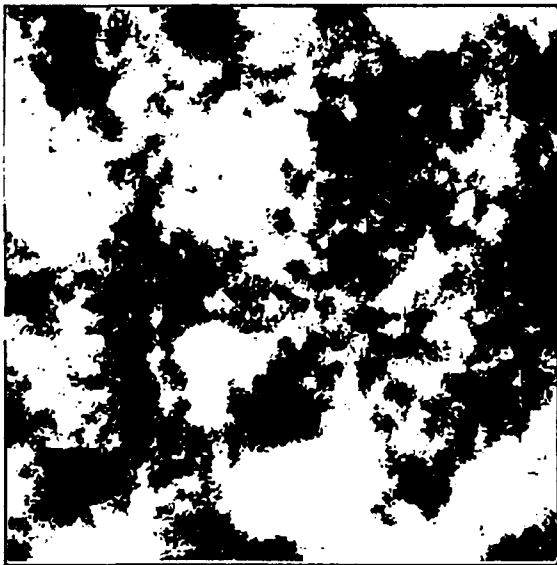


H=0.6

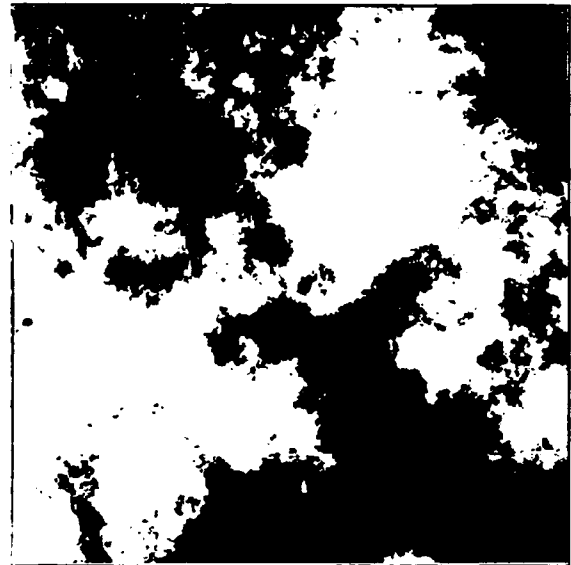


H=0.8

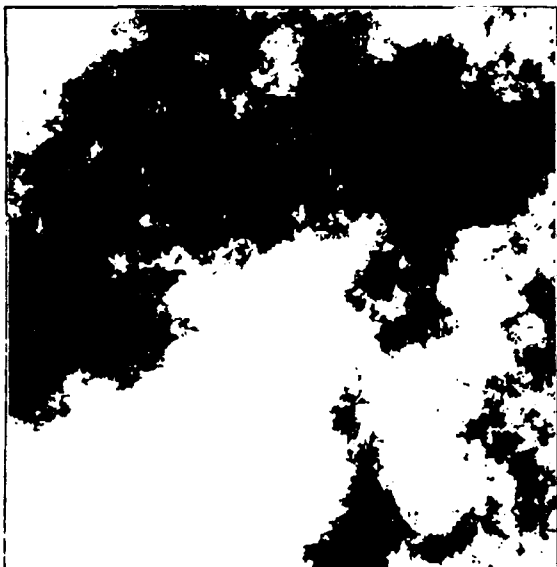
**Figure 17** Sequence of Binary Cloud Scenes (50% Cloud Cover) Generated with the Two-Dimensional SRA Method with Various Values for the Hurst Parameter ( $r = 0.5$ )



$r=0.2$



$r=0.4$



$r=0.6$

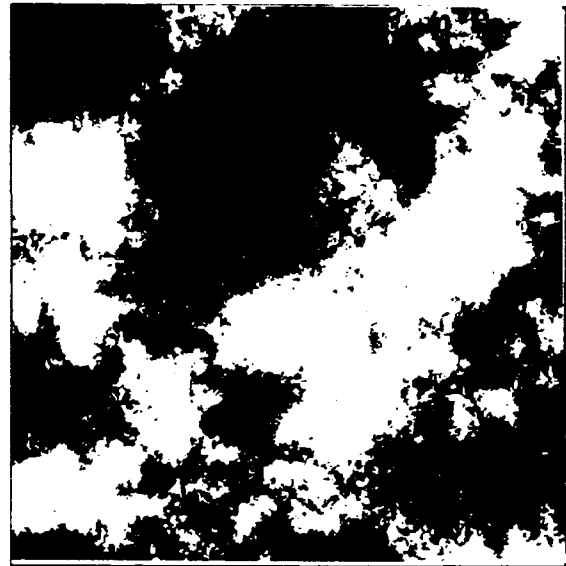


$r=0.8$

**Figure 18** Sequence of Binary Cloud Scenes (50% Cloud Cover) Generated with the Two-Dimensional SRA Method with Various Values for the Lacunarity Parameter ( $H=0.5$ )



Stratus



Stratocumulus



Cirrus

**Figure 19** Binary Cloud Scenes (50% Cloud Cover,  $10 \times 10$  km Horizontal Domain) Generated with the Two-Dimensional SRA Algorithms for Various Cloud Types

The prototype cirriform model, included in the interim model, allows for independent lacunarity parameter values in the x and y Cartesian coordinate directions. By using different r values along the axes, we are able to simulate fibrous-like cirriform clouds. Values used in the interim model for the Hurst and lacunarity parameters for each of the main cloud types are listed in Table 5. Future results, primarily from Task 3, may lead us to modify these values from their current defaults to better match observed cloud statistics.

*Generate Upper Cloud Surface* — Once the horizontal cloud/no cloud field is defined using the method outlined above, upper and lower cloud surfaces are built. In the interim model, we define the height of the upper surface at each grid point to be a function of the fractal field value at that point. In general, this method produces higher cloud tops toward the center of cloudy regions, where the fractal field generally has higher numerical value, and lower cloud tops toward the edges. This qualitative effect corresponds well to what we see frequently in nature.

We found that a function of the following form

$$\text{HGT}(x, y) = A \sqrt{(V(x, y) - V_{\min})} + \text{BASE} \quad (2.3-2)$$

where

$$A = (\text{TOP} - \text{BASE}) / \sqrt{(V_{\max} - V_{\min})}$$

BASE is the user-specified base height

TOP is the user-specified top height

$V_{\min}$  is the minimum field value

$V_{\max}$  is the maximum field value

**Table 5      Default Values for the Hurst and Lacunarity Parameters  
Used in the Generation of the Horizontal Cloud/No Cloud  
Field for Various Cloud Types**

	STRATUS	STRATOCUMULUS	CIRRUS	CIRROSTRATUS
H	0.7	0.5	0.4	0.6
$r_x$	0.4	0.2	0.5	0.5
$r_y$	0.4	0.2	0.3	0.3

produced visually realistic cloud top surfaces. Three sample cloud scenes generated using the improved horizontal distribution and upper surface generation techniques described here are shown in the next section.

### **2.3.3 Results And Conclusions**

The interim model incorporates many improvements within the general structure of the prototype model. Cloud scenes generated with the interim model appear qualitatively more natural and realistic than prototype model simulations. In Figs. 20, 21 and 22 we show simulated cloud scenes of various types: stratus, stratocumulus and cirrus, respectively. All are single-layer scenes with 60% fractional coverage extending over a 10 km x 10 km horizontal domain. These scenes were rendered by filling each voxel (i.e., volume grid point) with semi-transparent particles whose opacity is based on the water content in the voxel. Color is simulated using a simple shading model. We display the scenes as viewed

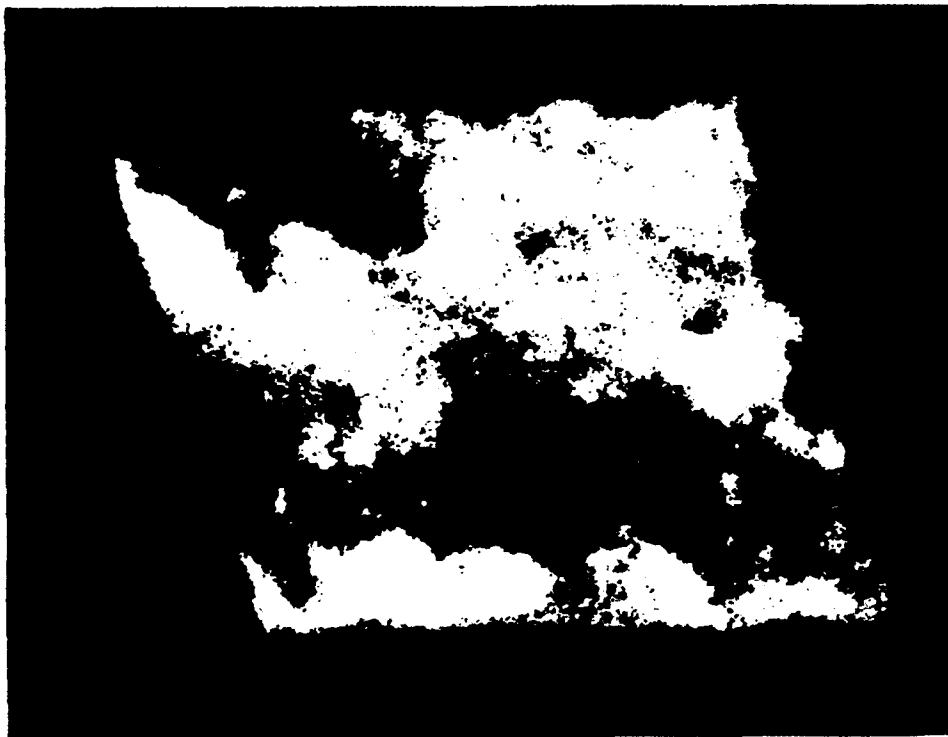


**Figure 20** 60% Stratus Cloud Layer Produced with the Interim Cloud Model



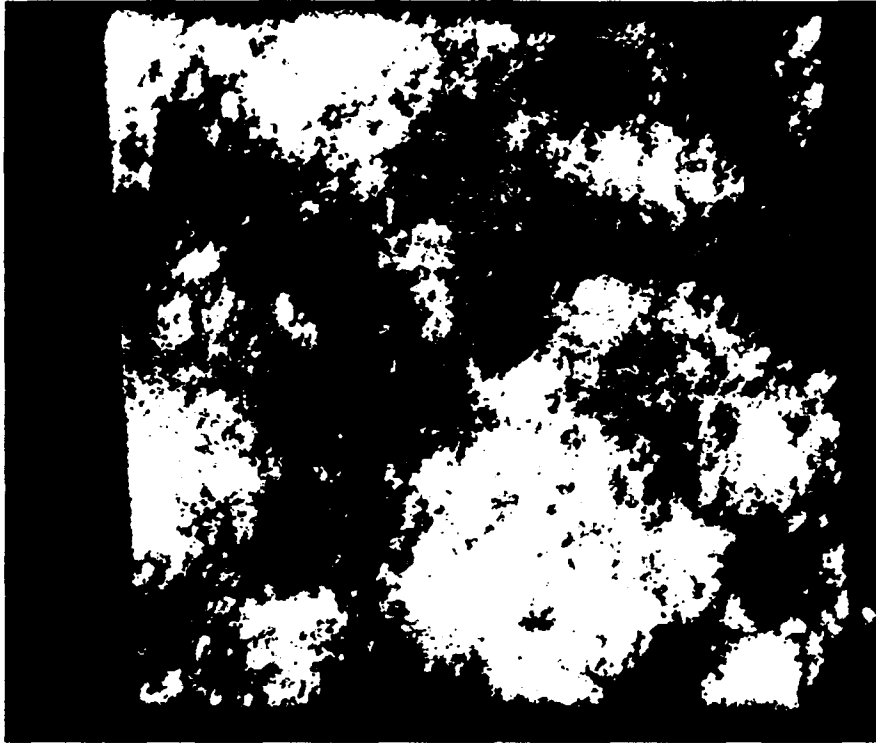


**Figure 21** 60% Stratocumulus Cloud Layer Produced with the Interim Cloud Model

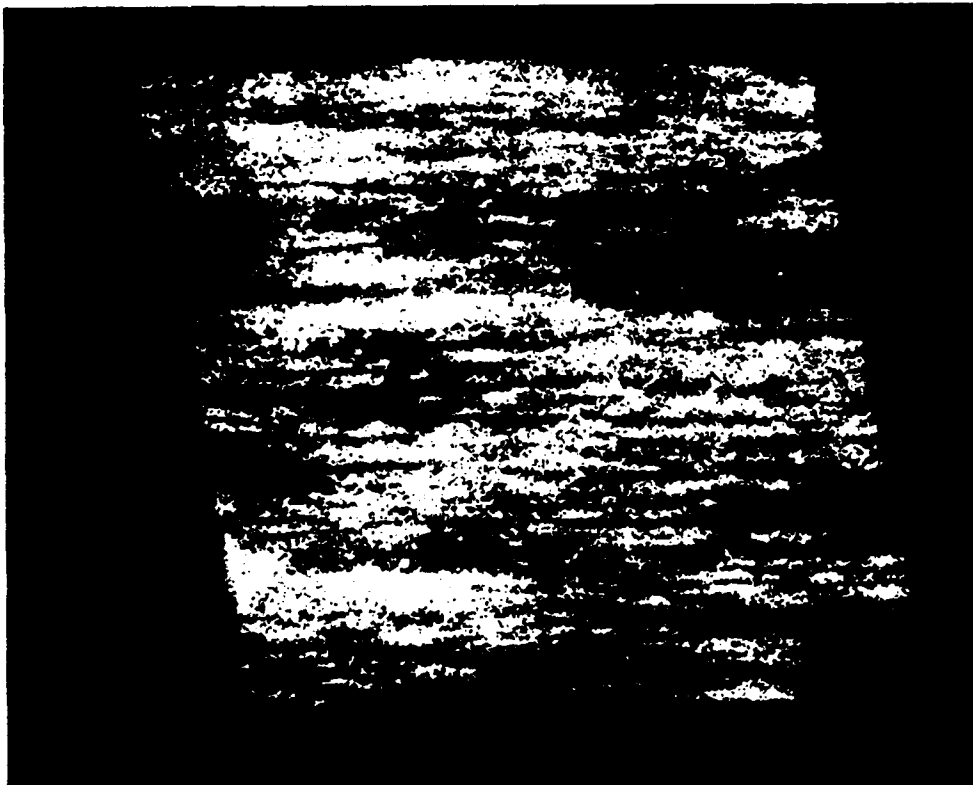


**Figure 22** 60% Cirrus Cloud Layer Produced with the Interim Cloud Model

from above and slightly off angle (similar to the view one would have looking out at clouds below from an airplane window) against a black background. Note the straight edges visible in the figures are the edges of the cloud model domain.

We can successfully simulate visually realistic stratiform clouds in the interim model (as in the first two figures). We are also able to produce non-isotropic cirriform clouds (Fig. 22). Currently, the prototype cirriform model simulates only the horizontal banded/fibrous nature of cirrus. It has no mechanism to treat the unique vertical structure so often visible (e.g., falling cirrus being swept by the wind). In the interim model, cirriform structure is developed in the same manner as stratiform, by building around the horizontal plane. Future efforts will include improvements to the cirriform model.

## **2.4 THE CLOUD SHADOW POST-PROCESSOR**

The presence of cloud shadows affects the energy budget at the earth's surface by modifying the heating and temperature. Therefore cloud shadows must be considered in surface energy computations. TASC developed the cloud shadow post-processor to compute a shadow map for a given ground domain, cloud scene and solar geometry. A description of the shadow post-processor is provided in this section.

The cloud shadow software package is written in standard FORTRAN 77. The package has been tested on a variety of Sun computers, a VAX/VMS 6310 and an IBM PC/AT. Figure 23 shows the relationship between the ground and cloud domains used in the shadow post-processor. The x-y center of the cloud domain lies directly above the x-y center of the ground domain. Typically the ground domain will be smaller than the cloud domain so that rays traced from the ground to the sun will pass through the cloud scene even for low solar angles.

### **2.4.1 Major Procedures**

An outline of the major procedures of the cloud shadow software package follows.

- Accept user input  
Request input parameters from the user in a simple question and answer format. Parameters include the size and resolution of the ground domain, name of the input cloud scene and output

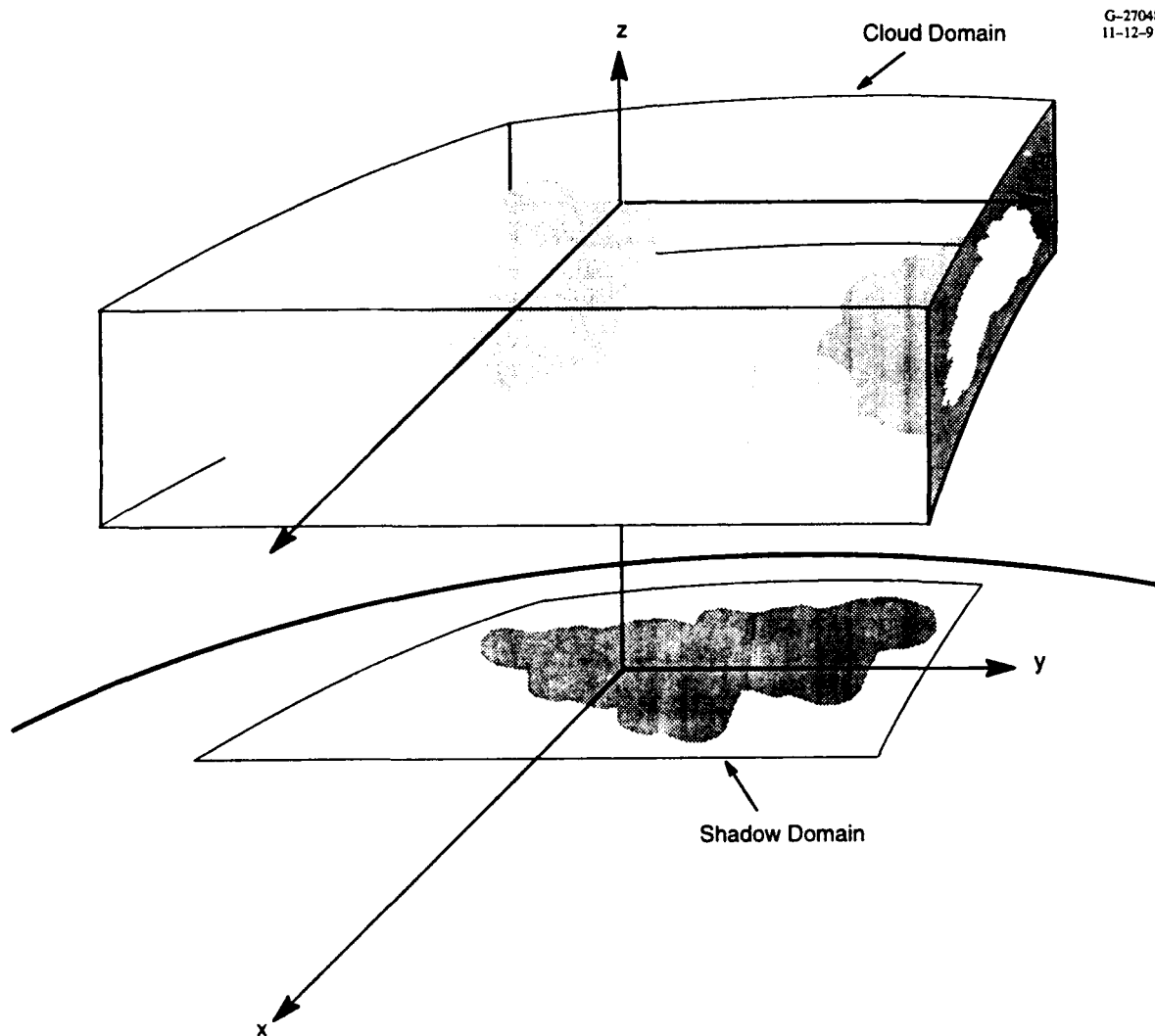


**Figure 23** Relationship of Cloud and Ground Domains in the Cloud Shadow Post-Processor

shadow map files, and solar angles. The user can specify the solar zenith and azimuth angles directly or give the date, time and location (which are then used to compute zenith and azimuth).

- Define solar zenith and azimuth angles

Compute solar position angles with respect to the latitude-longitude position of the ground domain for a given date and time (following methods in Ref. 14). If the user chooses to specify the solar zenith and azimuth angles directly, this module is not run.

- **Track solar rays through cloud scene**  
Trace a path from each gridpoint in the ground domain, through the cloud scene toward the sun. If a cloud element (a non-zero water density value) is found anywhere along the path through the cloud domain, the gridpoint on the ground is defined to be in shadow, otherwise it is clear.
- **Write shadow map to output file**  
Write the two-dimensional binary shadow map to the user-specified output file along with a header containing the size and resolution of the ground domain and the solar zenith and azimuth angles.

#### **2.4.2 Methodology**

The interim cloud model is capable of generating cloud scenes with a maximum horizontal extent on the order of 100 km by 100 km. For cloud scenes of that size the curvature of the Earth and the cloud domain must be taken into account when computing a ground shadow map. Rays are traced from every grid point in the ground domain along a line to the sun through the "curved" cloud region. As each ray is traced upwards through the cloud domain, the location of the intersection of the sun ray and the cloud domain is computed.

The point of intersection is computed for each vertical level in the cloud domain and is then converted to x-y-z grid coordinates. Using the direct-access cloud scene file as a look-up table, the volume element corresponding to the computed x, y, z location is retrieved. If the liquid water density within that volume element is non-zero (i.e., cloud exists at that point in space), the ground grid point is defined to be in shadow, and calculations for the succeeding ground grid point begin. If it is zero (i.e., no cloud exists at that point), the process continues to the next vertical level in the cloud scene. The process ends when a cloud element is found or when all vertical levels in every possible cloud layer have been traversed.

The x-y intersection point, computed for each vertical level in the cloud, is defined in terms of x and y offsets measured from the center of the cloud domain. Two components make up each of the x and y offsets. The first components ( $S_{x0}$  and  $S_{y0}$ ) depend on the position of the ground grid point as measured from the center of the ground domain. The second components ( $S_{x1}$  and  $S_{y1}$ ) take into account the angle that the sun rays make with respect to the ground domain. The total offset in each direction is the sum of the two components (see Fig. 24 for reference).

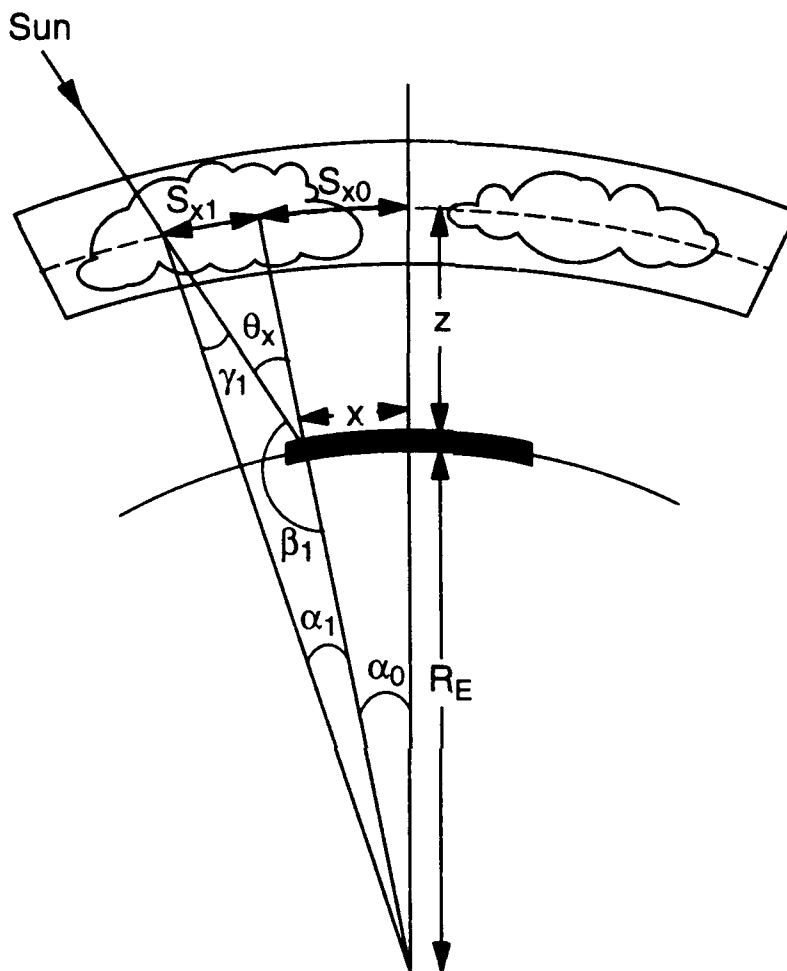


**Figure 24** X-Z Cross-Section Showing Variables Used in Cloud Shadow Calculations

Before computing the offsets in the two coordinate directions, the solar azimuth and zenith angles ( $\theta_a$  and  $\theta_z$ , respectively) must be reduced to Cartesian coordinates ( $\theta_x$  and  $\theta_y$ ), where  $\theta_x$  and  $\theta_y$  are the angular distance from zenith in the x and y directions, respectively (Fig. 25). The angles,  $\theta_x$  and  $\theta_y$ , can be computed by the following simple geometric relationships.

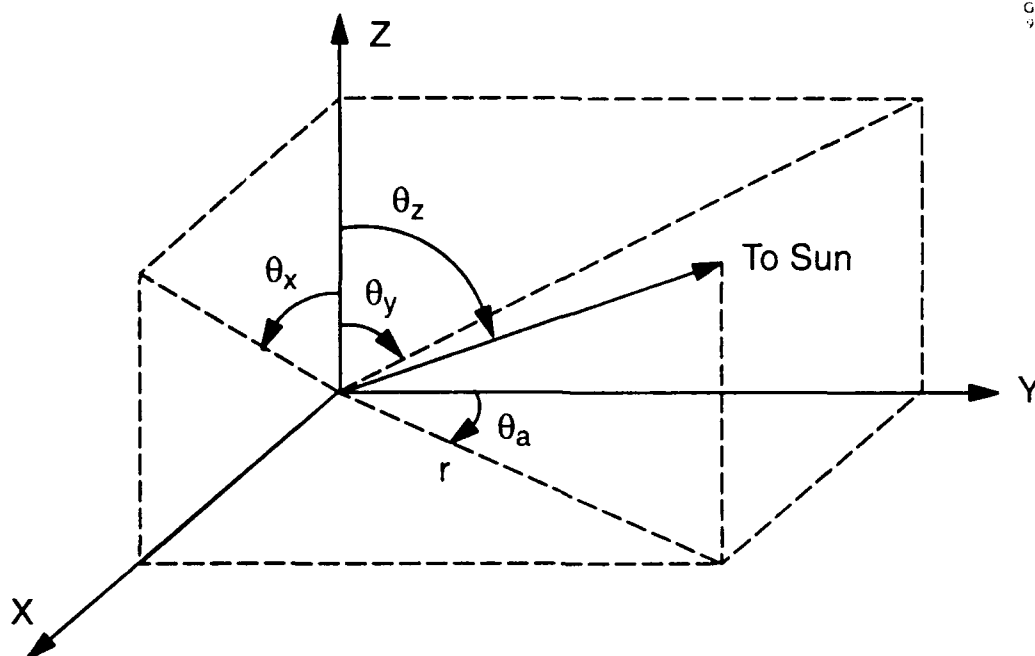


**Figure 25** Geometry Used to Convert Solar Angles to Cartesian Coordinates

$$\text{TAN } \theta_z = r/z \quad (2.4-1)$$

$$x = r \text{SIN} \theta_a \implies x = z(\text{TAN} \theta_z)(\text{SIN} \theta_a) \quad (2.4-2)$$

$$y = r \text{COS} \theta_a \implies y = z(\text{TAN} \theta_z)(\text{COS} \theta_a) \quad (2.4-3)$$

$$\theta_x = \text{ARCTAN}(x/z) \implies \theta_x = \text{ARCTAN} [(\text{TAN} \theta_z) (\text{SIN} \theta_a)] \quad (2.4-4)$$

$$\theta_y = \text{ARCTAN}(y/z) \implies \theta_y = \text{ARCTAN} [(\text{TAN} \theta_z) (\text{COS} \theta_a)] \quad (2.4-5)$$

A description of each of the two components which make up the total x and y offsets follows below. First, the offset due to the position of the ground grid point ( $S_{x0}$ ) is computed in the x-direction as follows (see Fig. 24):

$$\alpha_0 = x/R_E = \frac{S_{x0}}{(R_E + z)} \quad (2.4-6)$$

$$S_{x0} = \frac{x}{R_E} (R_E + z) = x \left( 1 + \frac{z}{R_E} \right) \quad (2.4-7)$$

where

$R_E$  = radius of the earth

$x$  = distance of the gridpoint from the center of the ground domain in the x-direction

$z$  = height of a level in the cloud domain.

The y offset ( $S_{y0}$ ) is computed in the same manner. The point corresponding to these offsets is the point that would be traversed if the sun was directly overhead. For cases in which the sun is not directly overhead a second contribution to the x and y offsets must be computed ( $S_{x1}$  and  $S_{y1}$ ). Using the law of sines and some simple geometry, the offset due to solar angle effects can be found as follows (we have outlined the calculations in the x-direction, similar results are found in the y-direction):

$$\beta_1 = \pi - \theta_x \quad (2.4-8)$$

$$\gamma_1 = \text{ARCSIN} \left[ \frac{R_E}{(R_E + z)} \text{SIN}(\beta_1) \right] \quad (2.4-9)$$

$$\pi = \alpha_1 + \beta_1 + \gamma_1 \quad (2.4-10)$$

$$\alpha_1 = \theta_x - \text{ARCSIN} \left[ \left( 1 + z/R_E \right)^{-1} \text{SIN}(\theta_x) \right] \quad (2.4-11)$$

$$S_{x1} = \alpha_1 (R_E + z) = (R_E + z) \left\{ \theta_x - \text{ARCSIN} \left[ \left( 1 + z/R_E \right)^{-1} \text{SIN}(\theta_x) \right] \right\}. \quad (2.4-12)$$

A multiplication factor based on the location of the sun is added to keep track of the sign of the offset. The total offsets due to both ground position and solar angle in each direction are:

$$S_{x\text{total}} = S_{x0} + S_{x1} \quad (2.4-13)$$

$$S_{y\text{total}} = S_{y0} + S_{y1}. \quad (2.4-14)$$

As previously noted, the offsets from the midpoint of the cloud domain at each level are converted to grid coordinates. The coordinates define an index into the direct-access file containing the multi-layer cloud scene. There are no limits to the resolution of the ground domain, except for limits on overall computational resources. In practice however, effective resolution on the ground is limited by the resolution of the cloud scene.

## **2.5 THE VISUALIZATION POST-PROCESSOR**

In support of the Engineer Topographic Laboratories as a SWOE demonstration participant, we developed the visualization post-processor to convert cloud model output fields (generated with the interim model) to a form acceptable for use in the Computer Image Generation (CIG) system at ETL. The cloud scenes generated with the interim cloud model are stored as three-dimensional arrays. ETL required that these arrays be converted to polygonally faceted surface representations for use with their CIG system. We use the marching cubes algorithm to perform this conversion (Ref. 15).

The marching cubes algorithm finds an approximate isosurface for the 3-d cloud data. The surface is specified as a list of triangles; each triangle is defined by a set of indices into a vertex list. The vertex list contains the spatial position of each vertex along with color information (i.e., grey-scale color) based on position with respect to the sun and attenuation effects for that vertex. We discuss the marching cubes algorithm in Section 2.5.1. In Section 2.5.2 we describe the technique employed to color each vertex.

### **2.5.1 The Marching Cubes Algorithm**

The marching cubes algorithm was developed for computed tomography (CTSCAN) data sets, which are composed of a three-dimensional volume of density samples. The algorithm steps, or "marches," through the data set one slice at a time, comparing eight density samples (i.e. the corners of a cube) against a user-specified threshold value. Each sample is classified as a "1" or "0" based on whether the density at that point falls above or below the threshold, respectively. (Samples with density equal to the threshold are also classified as "1"). The eight samples composing each cube (when classified as "0" or "1") define an 8 bit integer which is used as an index into a look-up table of precalculated polygonal facets for a cube (Fig. 26). There are 256 configurations of polygonal facets, which, when symmetry is accounted for, reduce to the 15 cases shown in Fig. 27.

The look-up table specifies each polygonal facet in a given index location as a list of edge indices. These edge indices correspond to the edges along which each vertex lies. The location of the vertex upon the edge is calculated via a direct linear interpolation between the two surrounding corners. This linear interpolation utilizes the density values at each corner as weighting factors.

The voxel data set is specified in an integer coordinate system based upon the number of samples in each of the x, y and z dimensions. As the algorithm marches through the



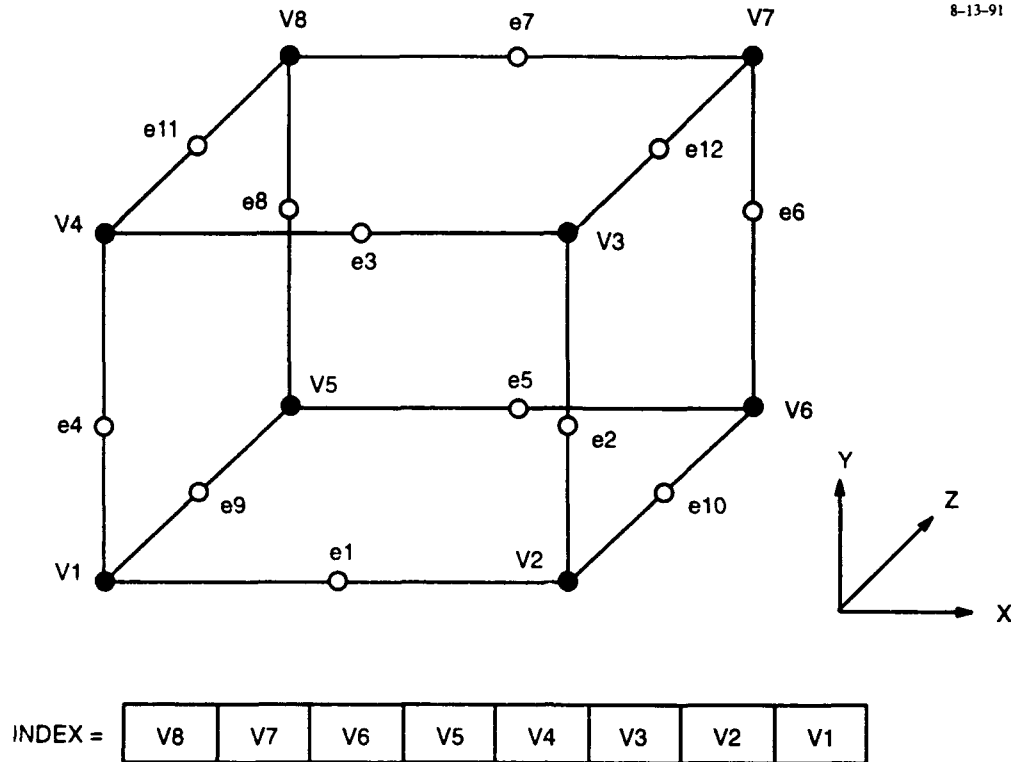


**Figure 26** Index Look-Up Table with Vertex Geometry Displayed for Reference (From Ref. 15)

data set it forms the cubes it processes from the samples found in two adjacent slices of data. Each edge from which the actual polygon vertex values are interpolated will be shared by up to four adjacent cubes. It is therefore possible to reduce the amount of work the algorithm performs by using a hash table storage technique. Each sample point, specified in its  $[i,j,k]$  integer coordinate space, can be thought to have three edges connected to it, one in each of the  $x$ ,  $y$  and  $z$  directions. By storing the  $[x,y,z]$  value of the polygon vertex calculated on a given edge in a sequential list, the index of that vertex can subsequently be stored in a hash table at a location calculated from the  $[i,j,k]$  coordinate of the associated sample point. The linear interpolation need not be performed again, the vertex index can simply be retrieved via a hash table look-up.

In addition to this efficiency improvement, certain additional calculations must be performed to account for anomalies in the data sets. The marching cubes algorithm assumes that slices are oriented so that no surface will lie directly upon the face of the cubes it builds from these slices. In our data sets this may not be the case. If the surface does lie

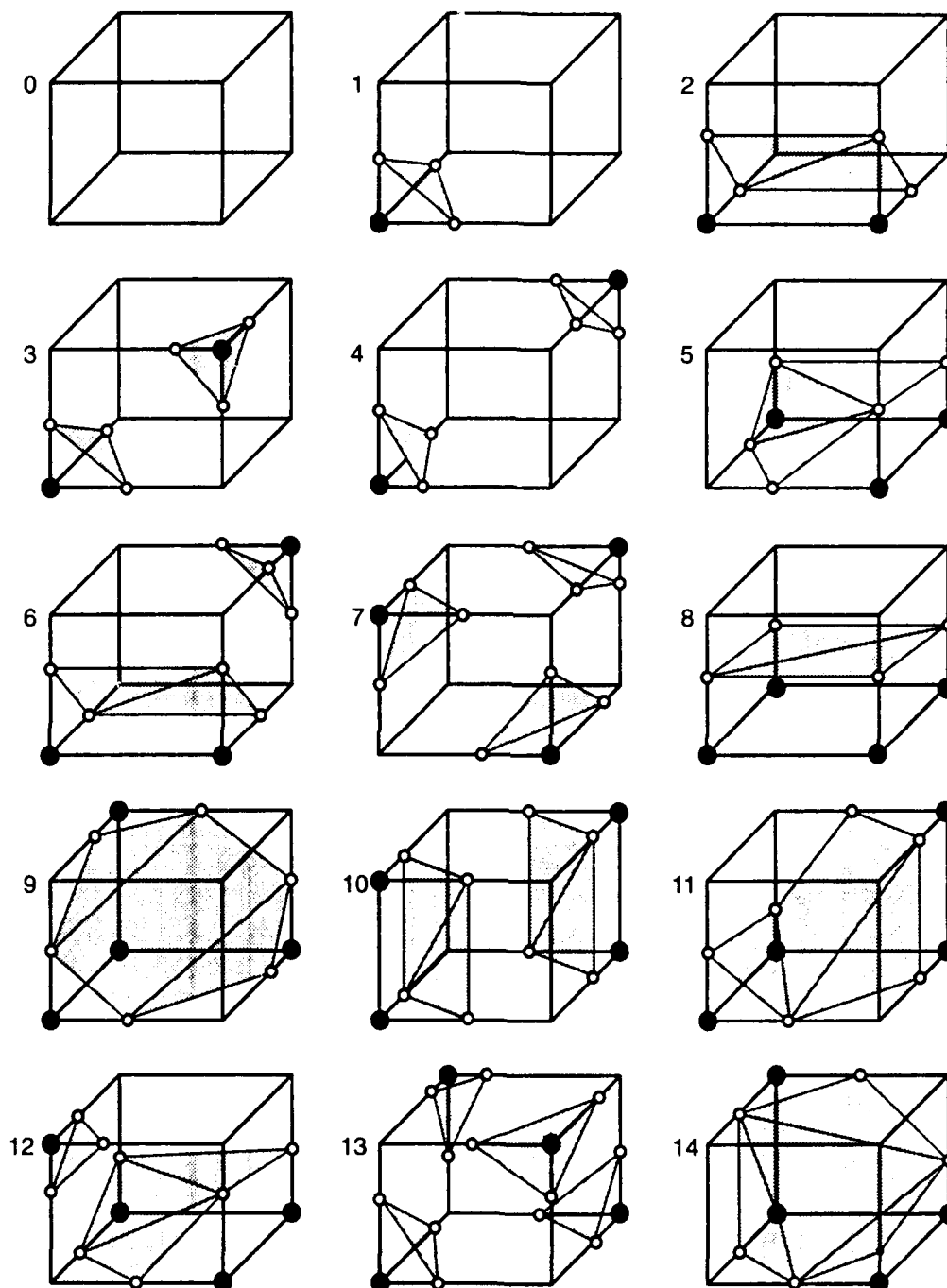


**Figure 27** The Fifteen Fundamental Polygonal Facet Representations. The Large Filled Circles Correspond to Points Within the Isosurface, and the Smaller Unfilled Circles Lie Outside the Isosurface (From Ref. 15)

along the face of the cube, additional polygons must be created along the face to insure surface closure. In the application of the marching cubes algorithm to cloud fields, we test for closure along the top and bottom vertical slices. First we find an average density value for the flat faces. Then, if the average value exceeds the specified threshold, additional polygons are specified using vertices already calculated for the configuration in question.

We have found that, in general, hundreds of thousands of polygons are required to approximate the complex cloud surfaces generated with the interim model. The CIG system is limited to approximately 30,000 polygons for any one geometry model. We can solve this problem by breaking the cloud domain into smaller pieces, each of which fits within the ETL polygon limit. Each portion can then be rendered independently.

### 2.5.2 Assigning Colors To Cloud Surfaces

The normal to the surface at each vertex is used to determine the color at the vertex. We compute the normal at each voxel in a pre-processing step by calculating the three-dimensional gradient of cloud water density at the voxel. When interpolation is performed to calculate the vertex locations, the gradient, also linearly interpolated, is calculated too. The unit surface normal at the vertex is simply the interpolated gradient divided by its magnitude.

After all vertices and polygons have been determined, an additional processing step is performed. First a base color for the vertices is specified by the user or set equal to a default value. Sun position is also determined from user input. The list of vertices is then traversed. For every vertex, the (x,y,z) position is retrieved and the associated (i,j,k) voxel is determined. From the position of the vertex and the position of the light source we calculate a light direction vector. Using this direction vector all voxels that lie between the current vertex and the light source are determined, and their liquid water density values are summed. If this sum is zero, then the vertex lies on a side of the cloud facing the light source, otherwise it does not. Figure 28 gives a graphical example of three vertex locations, their direction vectors and integrated path lengths through the cloud.

Color at each vertex is calculated as the default base color (generally bright white) less a certain amount of "darkening." Darkening is due to two effects: 1) surface normal shading and 2) attenuation within the cloud. Surface normal shading is a function of  $\vec{L} \cdot \vec{N}$  where  $\vec{L}$  is the light source vector and  $\vec{N}$  is the surface normal vector (Ref. 16). For

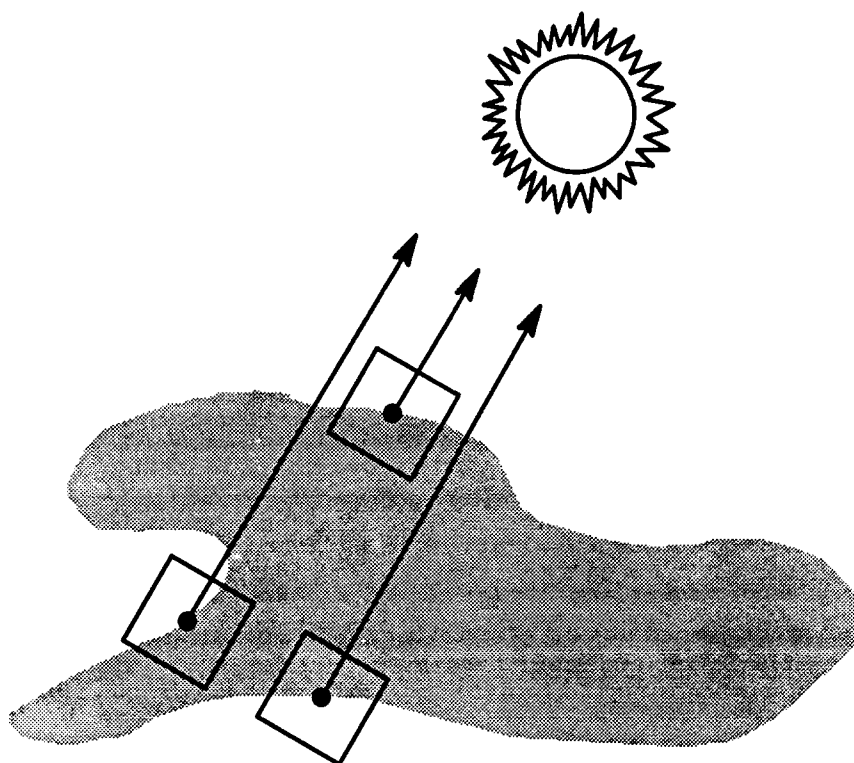


**Figure 28** Direction Vectors from Three Sample Vertices Through the Cloud Toward the Sun. Integrated Liquid Water Content Along each Vector is used in Color Computations

vertices that lie on a polygon which faces the light source (i.e., no cloud elements are between it and the light source), the amount of darkening is based on surface normal shading. Otherwise, darkening is based on the density sum. Cloud size, average voxel density and maximum voxel density are used to compute a "normalization factor." The integrated density along a vector from the vertex point to the light source is divided by the normalization factor to determine a percentage. The base color is then darkened by that percentage.

All vertices either face the light source or are obscured by some portion of the cloud. For vertices that are blocked by thin portions of the cloud the darkening is very slight and the color is relatively bright. For vertices that are on the farthest side of the cloud from the light source the darkening is greater. This technique results in very realistic cloud coloring as can be seen in Fig. 29 which shows a view from the ground looking up toward a cloud base. All of the grey-scale variations in this figure are due to attenuation through the upper portions of the cloud.

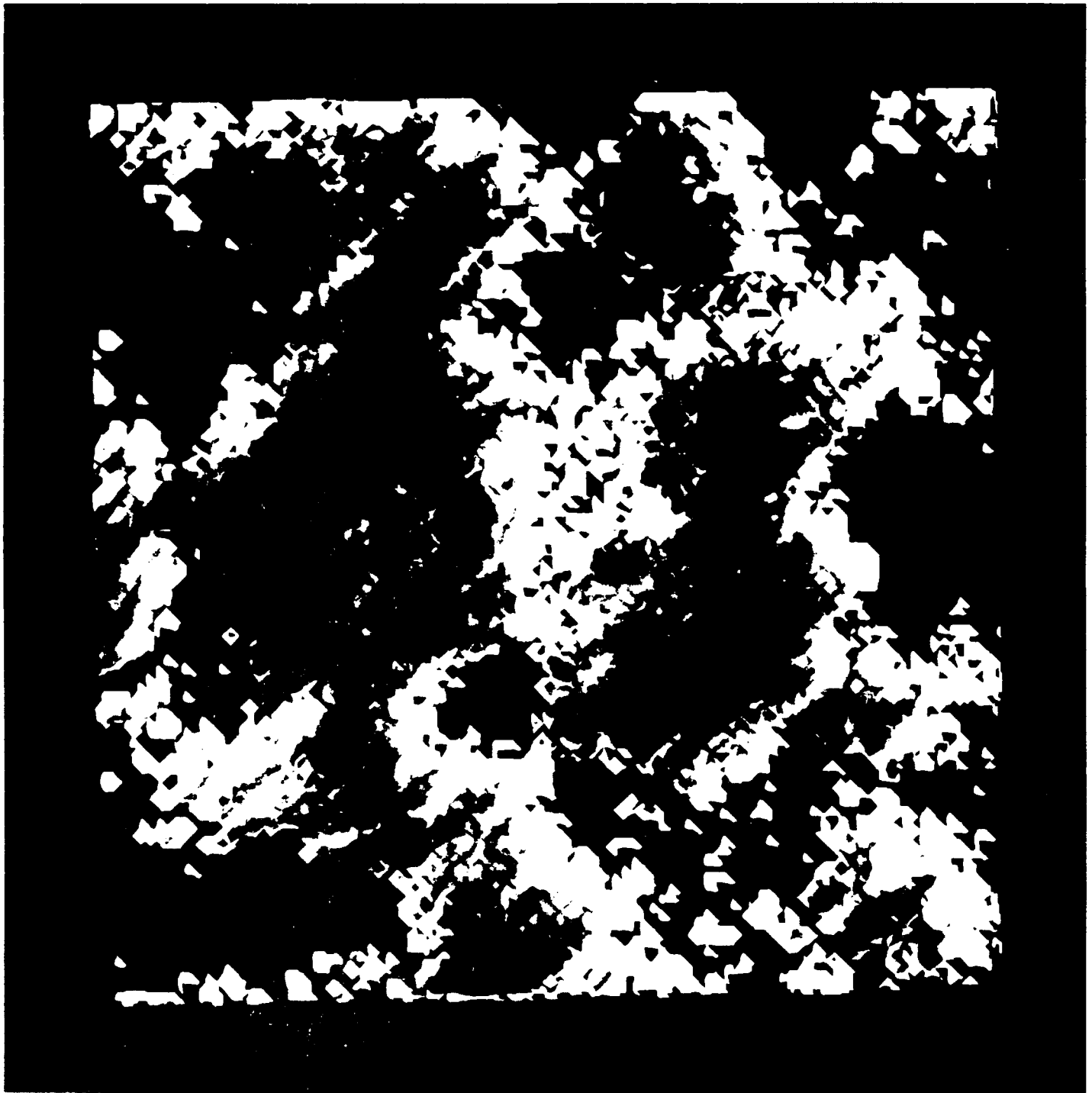


Figure 29      View from Below a 60% Stratocumulus Layer (10 x 10 km Horizontal Domain) Showing the Effects of Polygon Coloring due to Solar Azimuth and Zenith Angles Equal to  $45^\circ$

### **3. STATISTICAL ANALYSIS OF CLOUD DATA**

One important aspect of the Studies and Analyses task is the comparison of model-produced and observed liquid water density statistics. With sufficient observational data we can use maximum likelihood (and other) techniques to estimate model parameter values, evaluate the significance of the estimates, and (most importantly) evaluate the appropriateness of the SRA, BSW (and later, turning bands) models.

In this section we describe the SWOE demonstration locations for which environmental conditions will be simulated. We discuss the database of aircraft measurements available from the FAA for the surrounding regions, and describe the criteria used to select LWC series for use in parameter calibration. We present profiles of the aggregate cloud data as well as for individual cloud types. Finally we show results of a preliminary comparison of model-produced LWC series and measurements for two cloud types.

#### **3.1 CLOUD MODEL DEMONSTRATION SITES**

The cloud model is expected to simulate various cloud conditions at any location. The current SWOE demonstration location is Hunter-Liggett, California. Hunter-Liggett is located along the California coast, between Monterey and San Luis Obispo. This desert-like area is bounded on the north by the Coast Mountain Range and on the south and the west by the Santa Lucia Range. The area is dry during the summer with some rain in the winter. There is some marine influence along the western front due to the lower elevation of the Santa Lucia Range. These conditions also exist in areas such as southern France, southwest coast of South Africa and some other locations in California. One location which approximates this climatology, and for which there are extensive data available, is the Sacramento area which includes Auburn, Blue Canyon and Lake Tahoe. Auburn is located to the north of Sacramento, and Blue Canyon and Lake Tahoe are to the northeast. Auburn best approximates the Hunter-Liggett area, followed by Blue Canyon and Lake Tahoe. The latter two areas are higher in elevation with respect to Auburn. Lake Tahoe has the highest elevation and close to alpine climate conditions.

### 3.2 FAA DATABASE DESCRIPTION

Based on our survey, the FAA cloud database (formerly with the Naval Research Laboratory) is the most comprehensive and is reputed to be the best in the US. The data, originally obtained from various sources (digital tapes, tabular reports and journal articles), have been condensed in a standardized format. The database consists of time series of a variety of cloud-related variables along with averaged cloud data based on those series (described below). By analyzing the averaged variables, we were able to select a group of series to use in our comparison with model-produced LWC data.

The principal variables in the FAA database give information about the mission flight, cloud systems, prevailing weather and measurement related factors. Mission identifier variables include date, time, measuring agency, geographical location and surface elevation. Cloud information variables include cloud type, cloud group, cloud identification number, prevailing cloud distribution, cloud base and top heights and temperatures of cloud base and top. Weather variables include air mass information and coded descriptions of the weather conditions associated with the clouds under study. Measurement-related variables include the time duration (seconds) of the data sample, the distance (nmi) travelled by the aircraft, aircraft flight path (i.e., level, slant, spiral) during the sample, the type and intensity of precipitation, if any, observed at flight level from the aircraft or on the ground below the cloud under study and the state of the cloud particles sampled (water droplets, ice particles or both). The database also contains averaged variables such as air-speed (knots), altitude (feet), air temperature (deg C), LWC ( $\text{g/m}^3$ ) indicated by a hot-wire meter (Johnson-Williams or CSIRO-King), LWC computed from the droplet size distribution indicated by the FSSP (Forward Scattering Spectrometer Probe), median volume diameter ( $\mu\text{m}$ ) computed from FSSP droplet size distribution, droplet number density ( $\text{no/cm}^3$ ) indicated by the FSSP and particle number density ( $\text{no/liter}$ ) indicated by ice particle counters. The average LWC (ALWC) is the average of the measured and computed LWC (from the meter and the probe, respectively). Further information about the Johnson-Williams meter and the FSSP are given in Ref 17.

Each variable is averaged over continuous, uniform portions of the clouds. A set of rules has been established to define uniform cloud intervals. The rules are based on changes in air temperature, median droplet diameter, aircraft altitude, icing rate, droplet number density and the effect of snow or ice particles on the FSSP. The averaging interval

is described as follows. If the aircraft is still in continuous clouds at the end of the averaging interval, a new averaging interval is immediately started and continued until the next significant change in cloud properties occurs. Otherwise, the next interval begins when the aircraft enters another continuous cloud area. The advantages of this averaging scheme are listed below.

- Fixed intervals, e.g., one minute averages or averages over entire cloud passes are avoided.
- Averaging intervals are short enough to resolve any significant changes in cloud characteristics along the flight path.
- Averages remove extremes of particle mass concentrations or other variables.
- Averages preserve altitude dependent changes in cloud properties observed during ascents or descents through clouds.
- Broken or scattered cloud conditions as well as widespread continuous clouds are accommodated.
- Horizontal extent of continuous or semi-continuous icing conditions is available by summing the extents of consecutive averaging intervals.

### **3.3 SPATIAL SERIES DATA SELECTION**

To facilitate the selection of spatial series data sets, a preliminary statistical profile of the California data was taken. The measurements were taken over the Sacramento area during the winter months in the years 1979-80, 1982-83 in conjunction with an icing measurement program. The six cloud types include non-orographic stratus (St), stratocumulus (Sc), cumulus (Cu), and towering cumulus (Tc), and orographic cumulus (Orcu) and stratocumulus (Orsc). The statistical analyses used in data selection included:

- histograms of sample duration, altitude, ALWC and distance
- 3-d bar plots of cloud base and top heights and ALWC
- scatter plots of altitude and ALWC.

Figure 30 shows the California data profile which includes all six cloud types. Duration is in units of seconds, distance in nautical miles, altitude in 100's of feet, ALWC is given in  $g/m^3$  and count is the sample frequency of occurrence. To better accommodate the dynamic range of the plotting routine used to generate Fig. 30, we transformed cloud base and top heights and ALWC by the following:



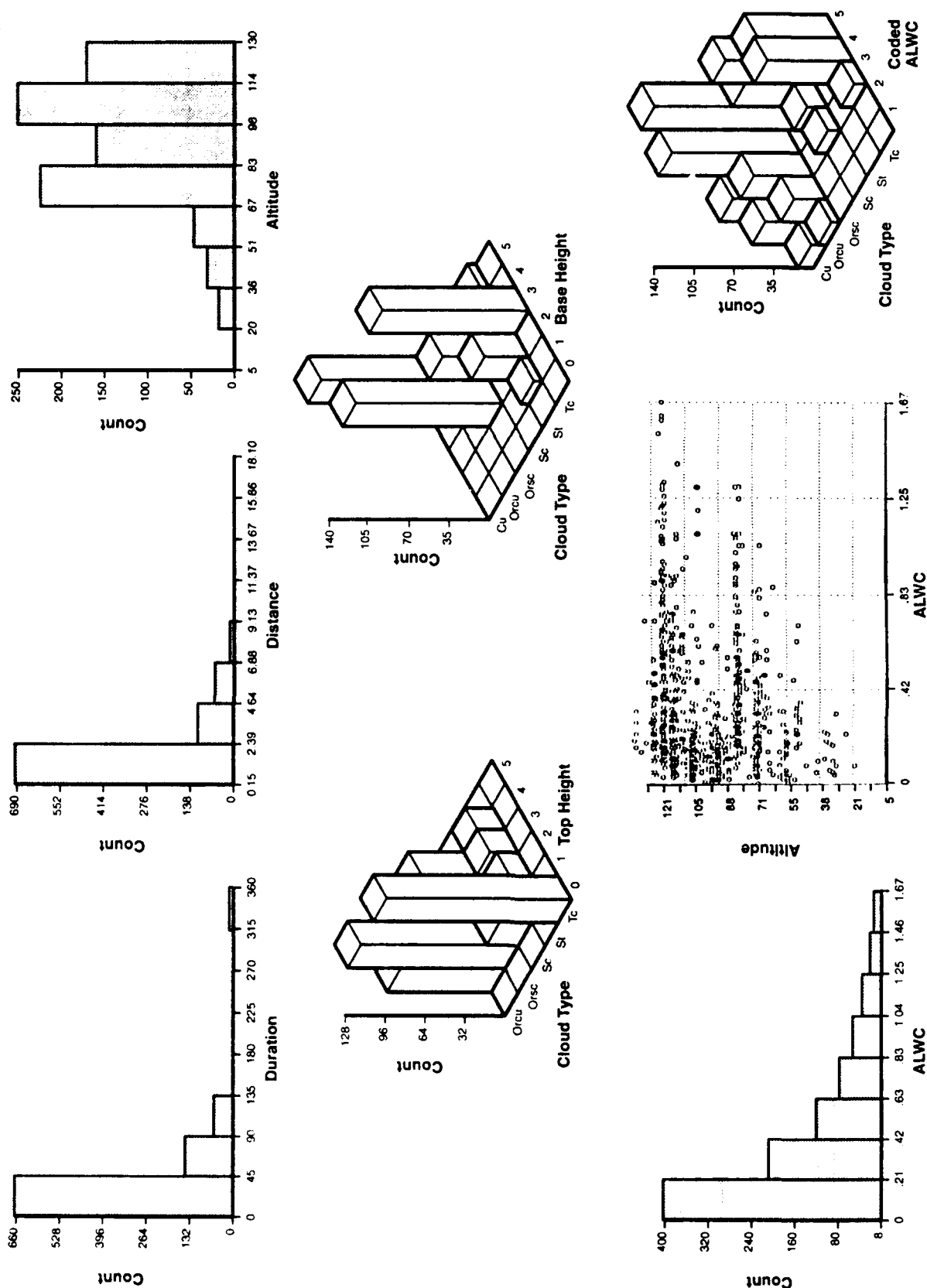


**Figure 30** Data Profile of All Cloud Types Measured in Northeastern California During February to March 1979-1983

- Cloud top and base heights

$$\text{coded HT} = 5 - \text{INT} \left\lfloor \frac{5\text{HT}}{\text{HT}_{\max} - \text{HT}_{\min}} \right\rfloor \quad (3.3-1)$$

- Cloud ALWC

$$\text{coded ALWC} = 5 - \text{INT} \left\lfloor \frac{5\log(\text{ALWC} + 1)}{\log(\text{ALWC}_{\max} + 1) - \log(\text{ALWC}_{\min} + 1)} \right\rfloor \quad (3.3-2)$$

These transformation equations allow the 3-d bar plots to be viewed from the higher valued interval (lower frequency of occurrence) to lower valued interval (higher frequency of occurrence). In most cases, this scheme provides a clear line of sight of most of the data in the plot. Ambiguities are clarified in the individual 3-d bar plots that follow in Figs. 31 through 36.

As shown in Fig. 30, most of the series are of relatively short duration (on the order of seconds). The distance travelled by the aircraft in these cases varies from about 0.15 nmi to 2.4 nmi, although there are a few cases in which the distance travelled is relatively long (7 nmi - 18 nmi). Most cloud altitudes fall between 6,700 ft to 13,000 ft. Because there is no information on the top height for cumulus, only five cloud types (of the six mentioned above) are represented in the 3-d bar plot. The cloud ALWC values vary from 0.0 - 1.67 (g/m<sup>3</sup>); the lower ALWC values occur more frequently. The Cu and Orcu cloud types have a more even distribution of ALWC. Figures 31 to 36 present the data profiles for each cloud type. These figures are useful during comparative analyses.

The criteria for spatial series data selection are as follows:

- different cloud types
- long sample duration
- cloud ALWC variations
- cloud altitude variations
- aircraft level maneuver.

For each cloud type, scatter plots of ALWC and altitude versus duration were made. Based on these scatterplots, we selected a number of spatial series that best met the criteria listed above. Scatter plots for Orcu are shown in Fig. 37 where we have highlighted the

G-23813-TR  
4-25-91

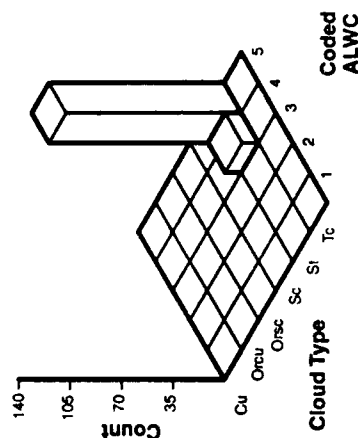
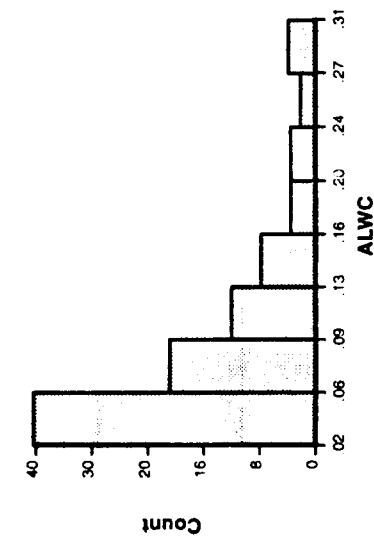
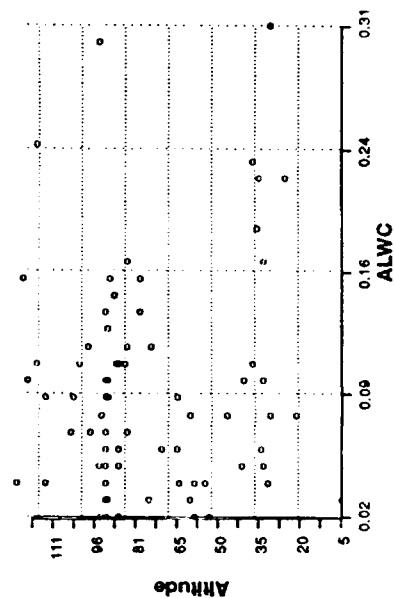
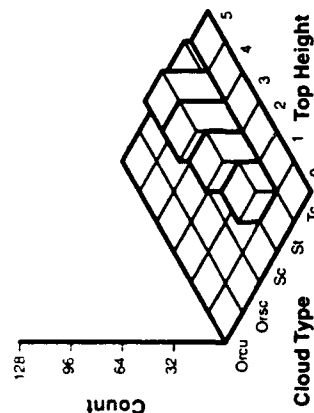
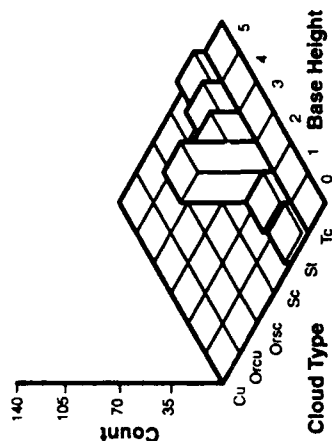
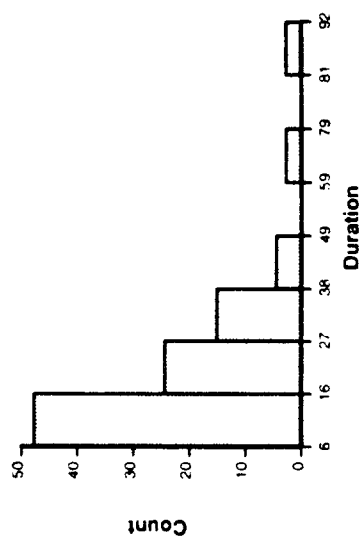
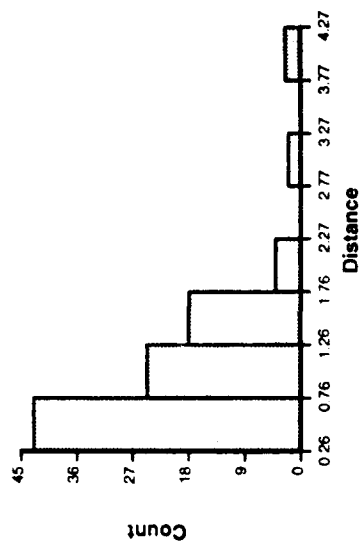
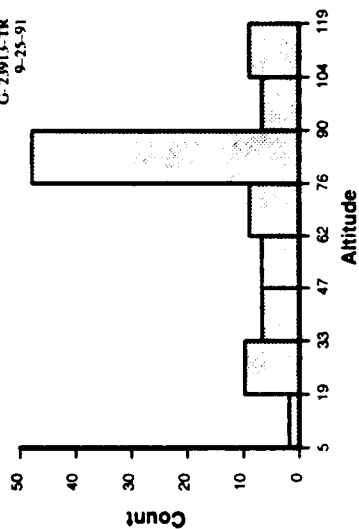


**Figure 31** Data Profile of Stratus (St) Clouds Measured in Northeastern California During February to March 1979-1983

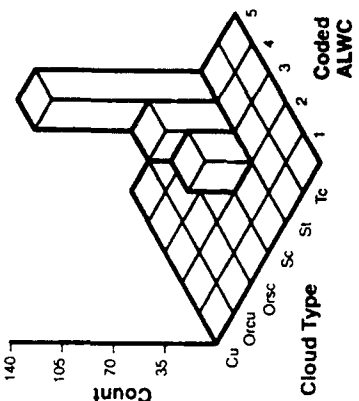
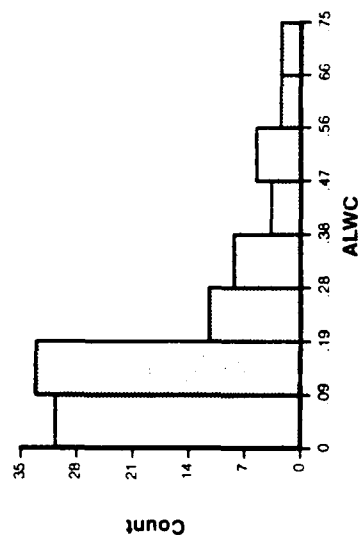
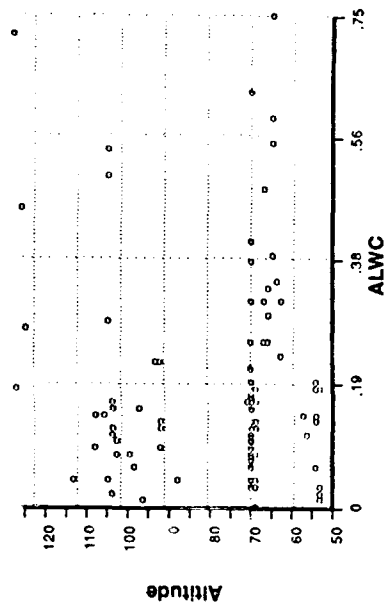
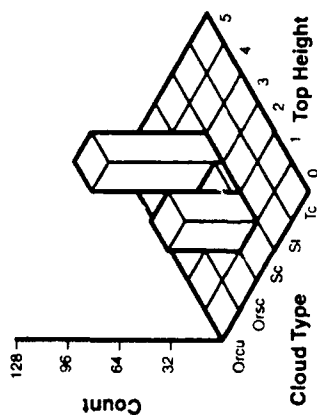
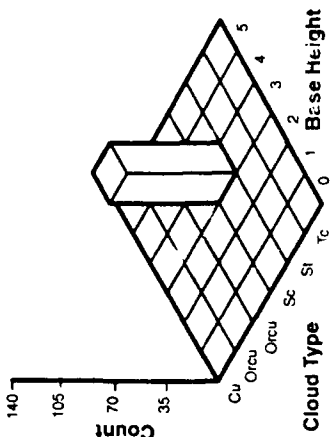
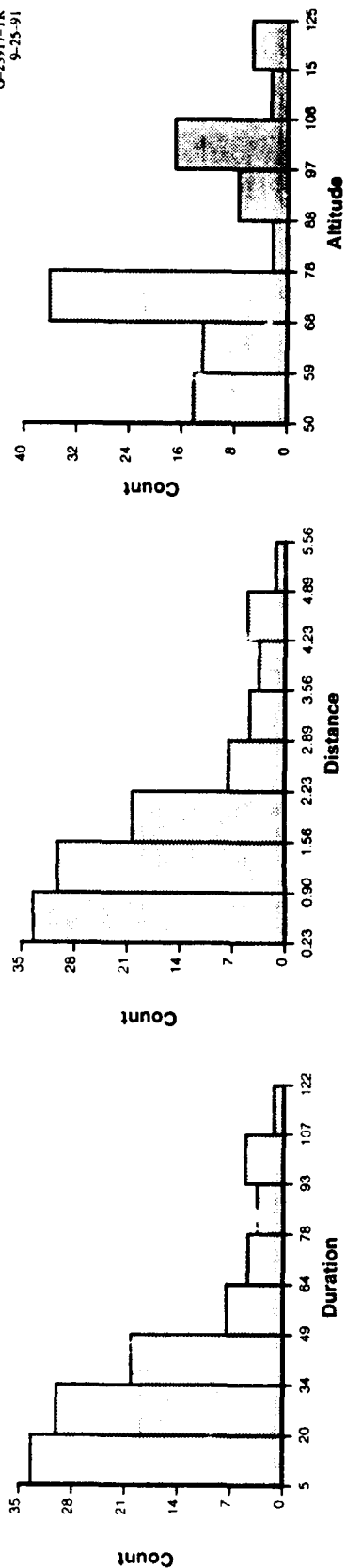


**Figure 32** Data Profile of Stratocumulus (Sc) Clouds Measured in Northeastern California During February to March 1979-1983

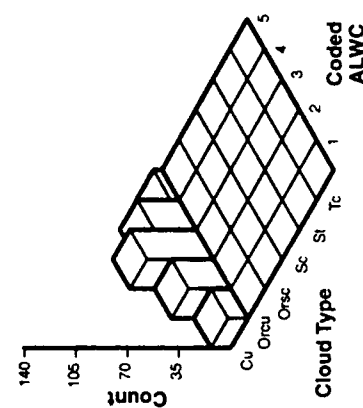
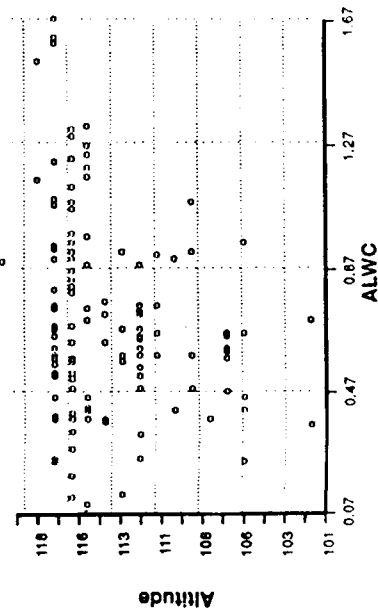
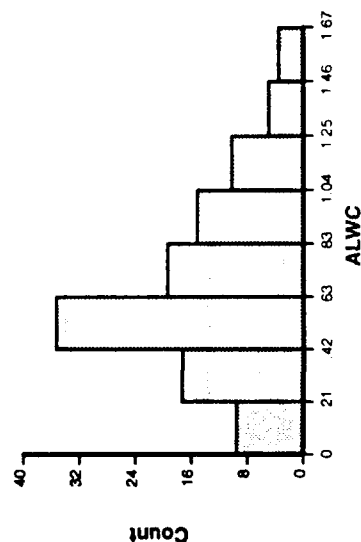
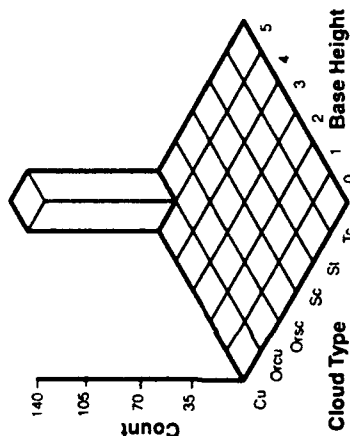
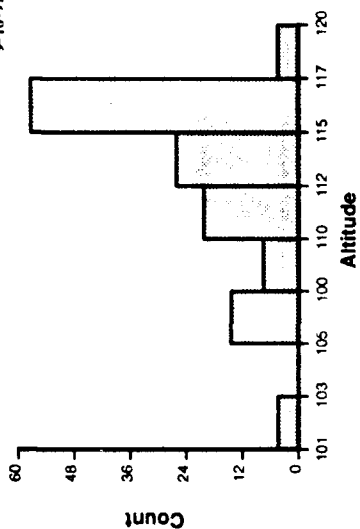
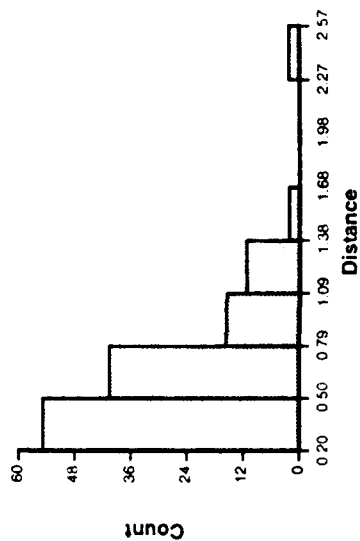
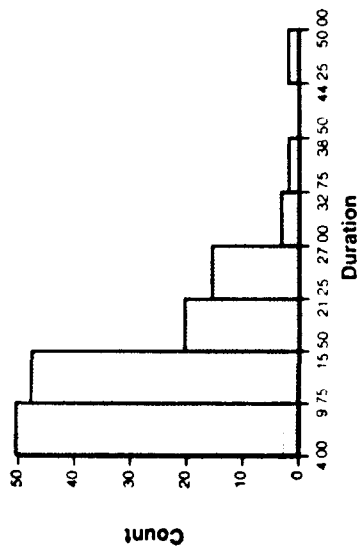


**Figure 33** Data Profile of Cumulus (Cu) Clouds Measured in Northeastern California During February to March 1979-1983

G-23915-TR  
11-22-91

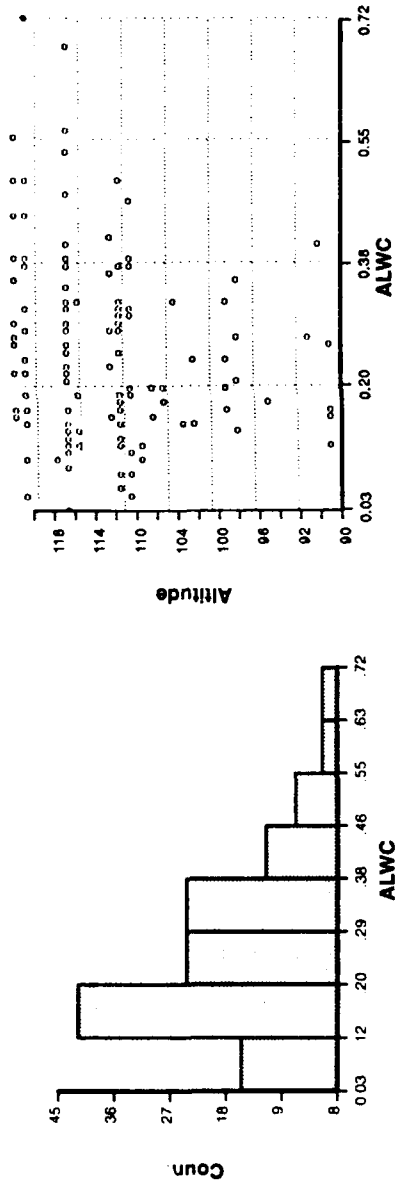
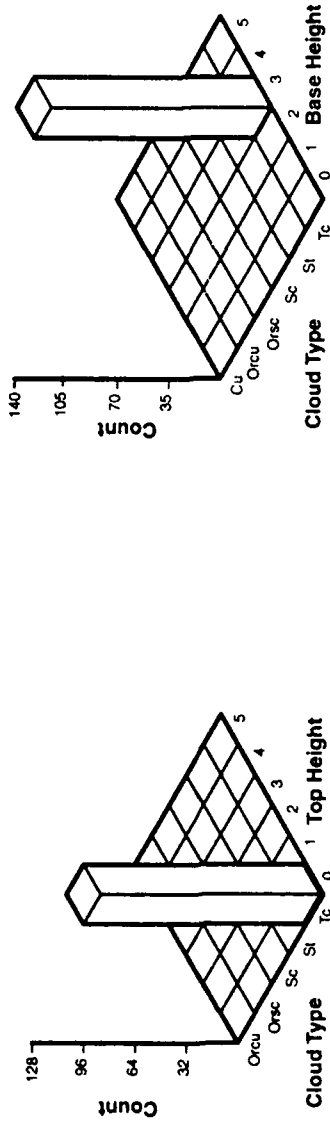
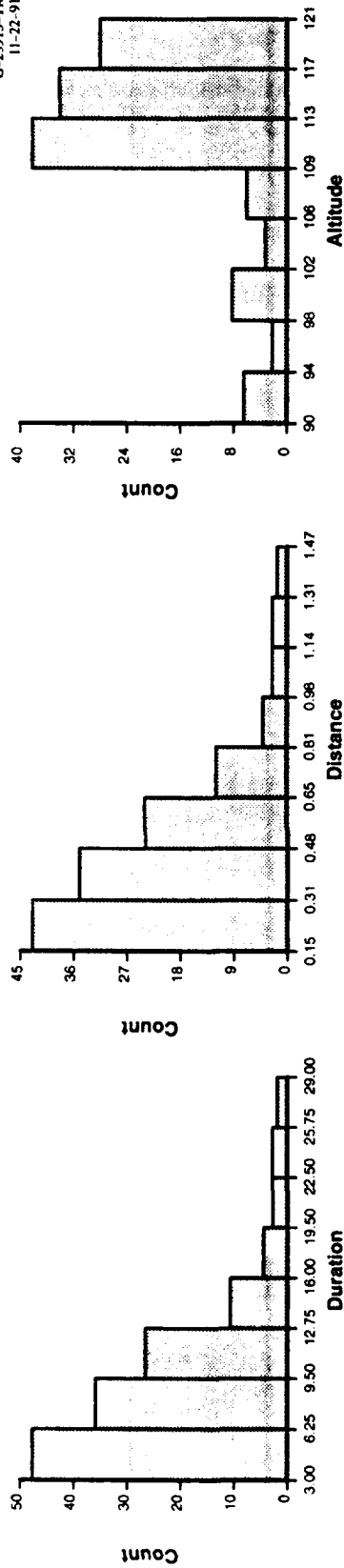


**Figure 34** Data Profile of Towering Cumulus (Tc) Clouds Measured in Northeastern California During February to March 1979-1983

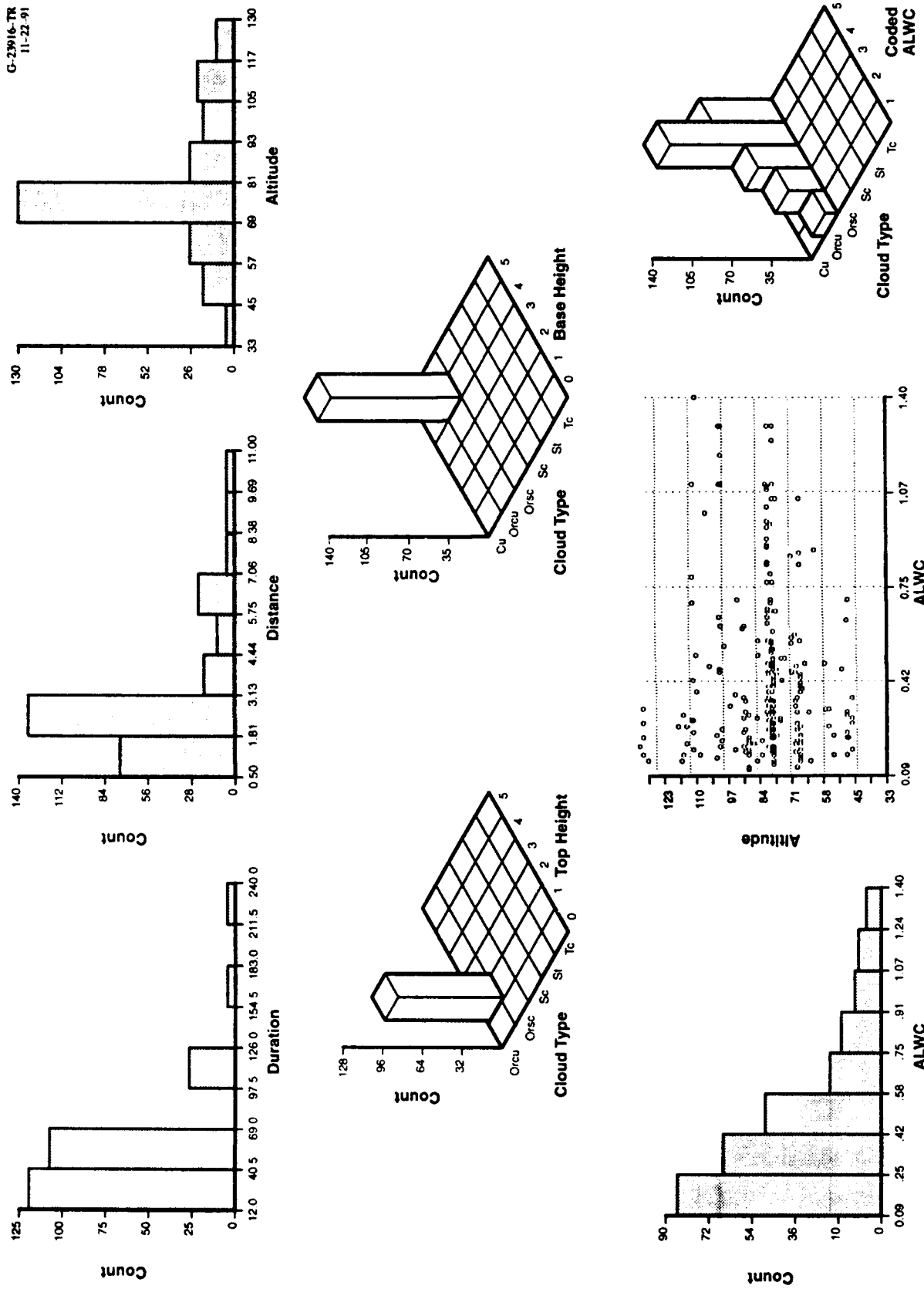
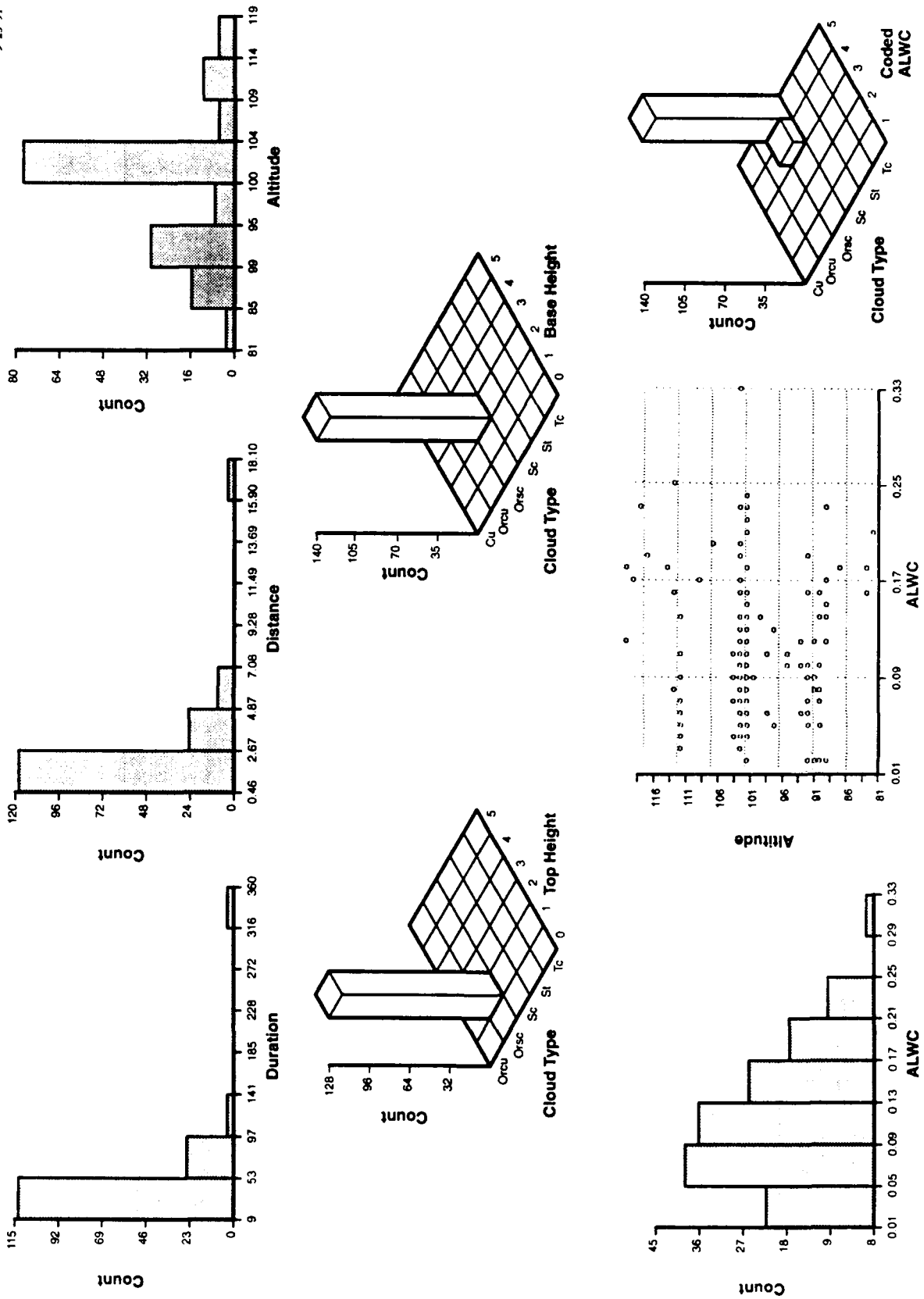


**Figure 35** Data Profile of Orographic Cumulus (Orcu) Clouds Measured in Northeastern California During February to March 1979-1983





series that were selected. The overriding criterion for selection is long sample duration. Among the long duration data sets, we chose series with level flight paths and varying ALWC and altitude. With the aid of scatter plots similar to Fig. 37 for each of the cloud types, twenty two data sets (at least three for each cloud type) were ordered from the FAA.

G-23918  
9-16-91

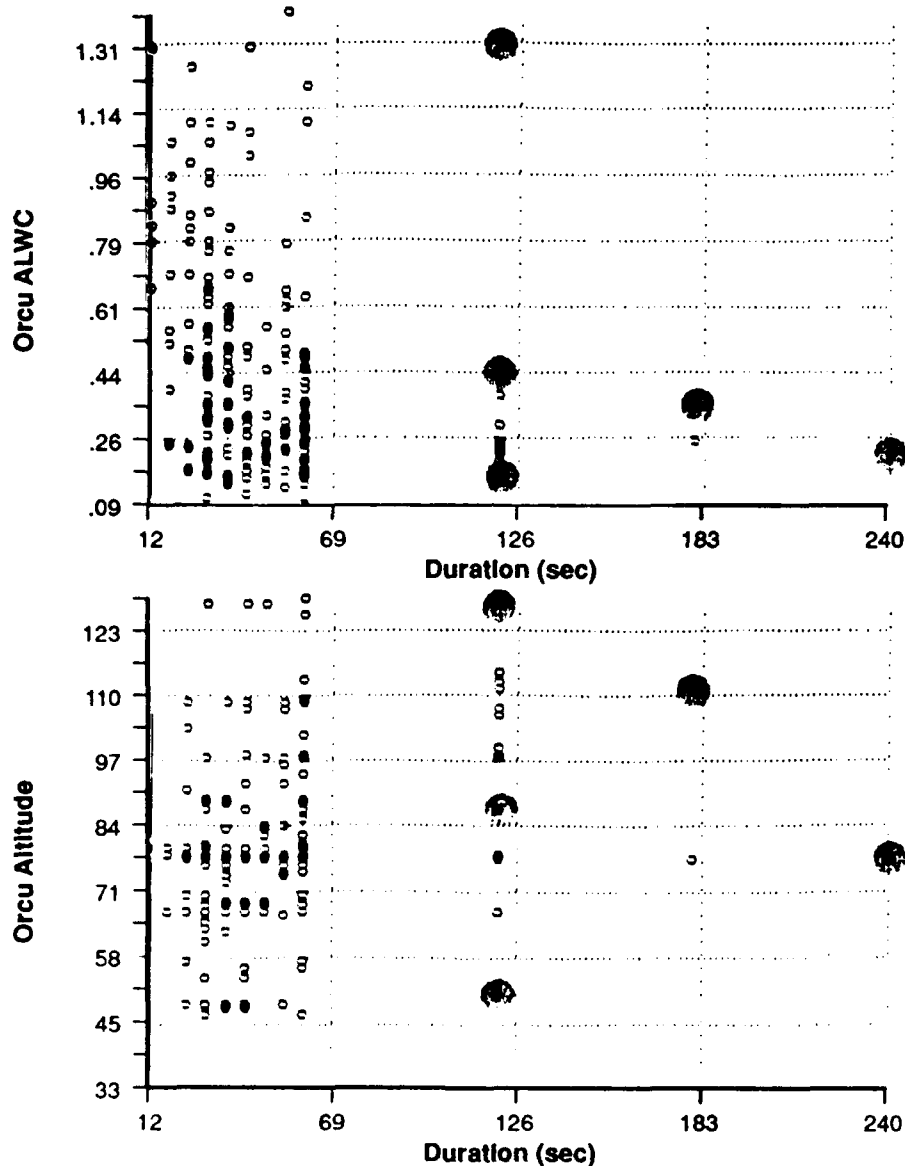


**Figure 37** Sample Scatter Plots Used in Data Selection Process (This Example For Orcu Cloud Type). Datasets with Longest Duration at Various ALWC and Altitude Values were Selected

### 3.4 COMPARISON OF ONE-DIMENSIONAL SPATIAL SERIES

In this section we present results of our comparison of observed and synthetic cloud water data using standard time series analysis tools. We have limited our initial analysis to St and Orsc (corresponding to Sc in the interim model) cloud types. For the comparison, we simulated cloud fields having the same physical characteristics (top and base heights, spatial resolution, etc.) and extracted horizontal (i.e., level paths) from various locations in the output field. Figure 38 shows observed LWC series side by side with corresponding modeled series (generated with the SRA model) for both St and Orsc cloud types. Qualitatively, the modeled and measured series are very similar. (One should note that the large visual difference between the two cloud types is partly due to the difference in series length. The Orsc series is almost 4 times the length of the St series.)

In the example in Fig. 38 we have chosen the mean and standard deviation of the modeled LWC to correspond to the exact observed statistics. We calculate the Hurst parameter from the observed series using the box-dimension algorithm (Ref. 3) which estimates the fractal dimension of the series. Estimates for the lacunarity parameter are based on trial and error. The curves shown in Fig. 38 are typical of the numerous series we have studied to date.

A key tool in our analysis (specifically for the estimation of the lacunarity parameter) is the autocorrelation function (ACF). The sample ACF is defined as

$$ACF(lag) = \frac{1}{\sigma^2} \frac{1}{N} \sum_{t=lag+1}^N (lwc_t - \langle lwc \rangle) (lwc_{t-lag} - \langle lwc \rangle)$$

where

- $\sigma^2$  = variance in the sample data
- $N$  = number of data points in the series
- $\langle lwc \rangle$  = mean liquid water content
- $t$  = time (space) index.

In Fig. 39 we include the empirical and model autocorrelation functions corresponding to the series in Fig. 38. Again we see very good qualitative agreement (typical of the numerous series we looked at) between the measured and modeled functions.

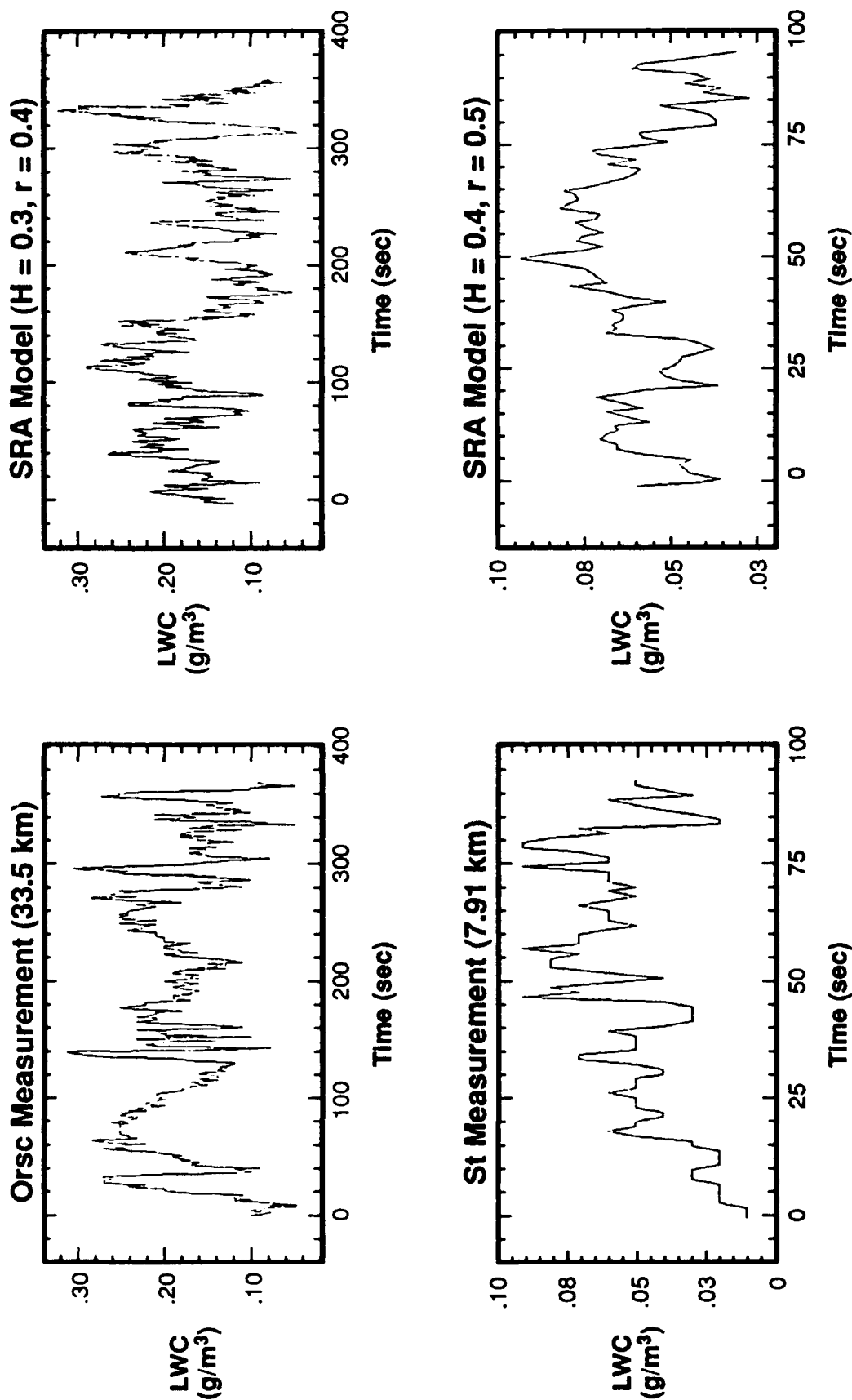


**Figure 38** Observed (using FSSP) and Corresponding Modeled LWC Spatial Series for Orsc and St Cloud Types

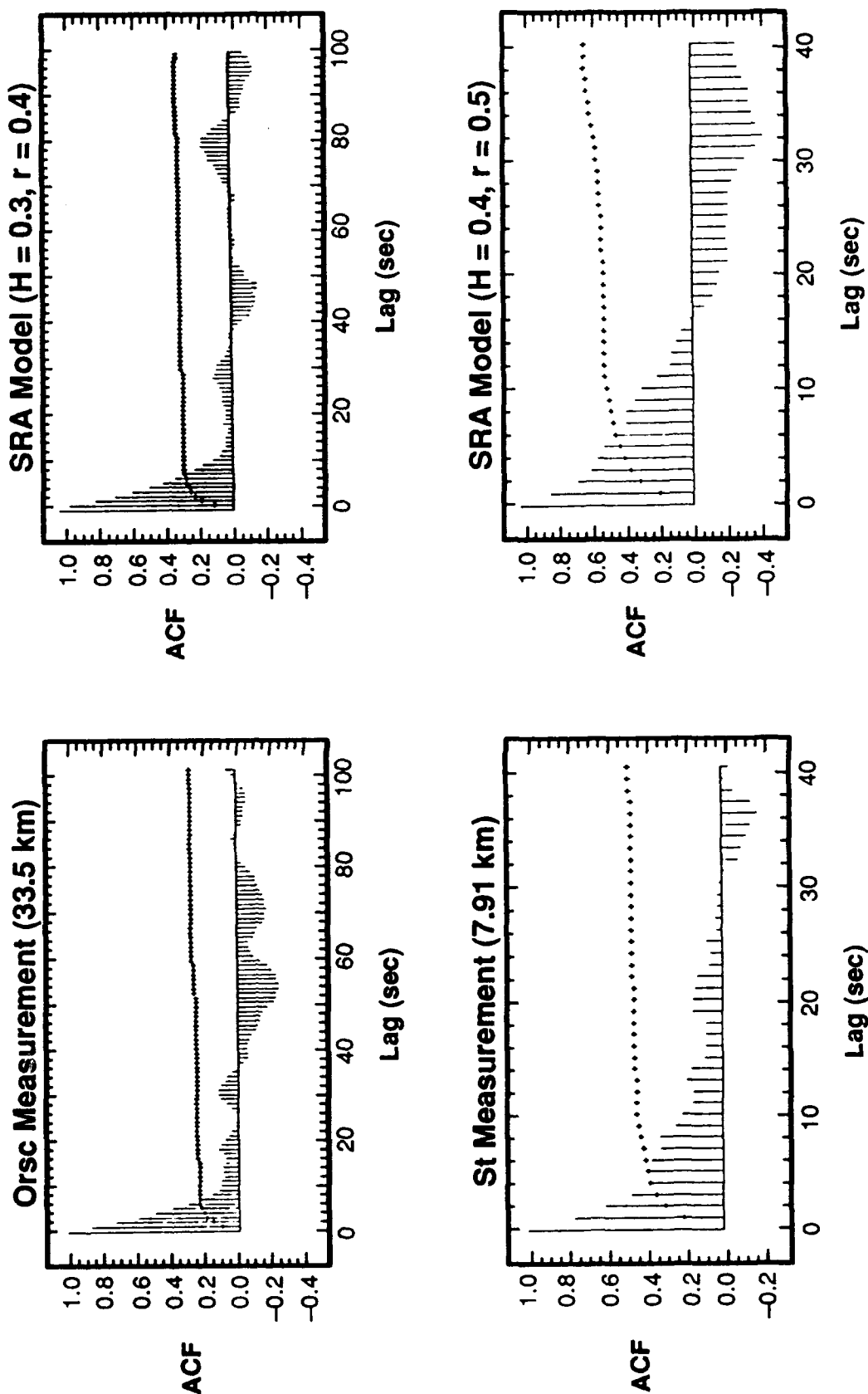


**Figure 39** Autocorrelation Functions for the LWC Spatial Series in Fig. 38

Due to the short length of many of the observed series, and the small overall number of available series, our conclusions are only qualitative; the SRA model (with suitable parameters) can be used to simulate clouds with horizontal variability and correlation structure characteristic of the measured lwc data sets. Ideally we would like to continue this analysis to test for the suitability of the SRA algorithm to model the vertical variations in LWC. The very limited number and overall duration of the slant path data sets make this analysis impossible at the current time. We are confident however, that we can model variations in the mean LWC as a function of height following Feddes' model (Ref. 7).

## **4. SUMMARY AND FUTURE PLANS**

### **4.1 SUMMARY**

The interim cloud scene simulation model, developed under the BTI/SWOE program, is an efficient and portable tool to generate multi-layer cloud scenes containing cirriform and stratiform cloud types (cumuliform will be included in the enhanced model). Cloud scenes consist of a 3-d field of LWC values, and may be used as input to other SWOE models such as those for thermal and radiative transfer. Development of the enhanced cloud model is currently underway and will include additional capabilities as discussed below in Section 4.2.

In this report we have described the design and development of the cloud scene simulation model. We have outlined the major model processes, including a description of the SRA fractal algorithm which is the basis of the model. We have also shown results of a comparison of model data and actual LWC measurements. Though more analysis is desired, early results are promising, showing very good qualitative agreement between spatial series extracted from several datasets. We conclude, in the following sections, with a discussion of plans for future work both in model development and evaluation.

### **4.2 THE ENHANCED MODEL (VERSION 3.0)**

The prototype and interim models were designed specifically to provide a platform for algorithm testing and development, and to encourage feedback early in the project from others in the SWOE community. Both models include the most fundamental functions of the cloud model: to generate the horizontal distribution of cloud elements, their vertical structure and their internal LWC distributions. Over the development period we identified both strengths and weaknesses in the model and its algorithms and we have changed the design accordingly. The enhanced model will include all of the fundamental functions of the two previous versions (suitably modified) along with a number of additional capabilities.

Three additional capabilities are currently being implemented: a cumuliform cloud model, temporal evolution, and a variable resolution grid. The cumuliform model will be

based in part on convection physics. The evolution capability will feature both advection of clouds by layer average winds and stochastic evolution (growth, change and decay) of cloud elements. Differential advection of adjacent layers will permit and accommodate vertical wind shears. Stochastic evolution will be achieved by adding a fourth (temporal) dimension to the SRA algorithm. The other new design feature, non-uniform grid resolution, will provide the maximum resolution where it is needed most, in the vicinity of the sensor. Near the horizon the resolution will be lower.

### **4.3 EVALUATION OF FIELD ALGORITHMS**

Throughout the course of model development we have evaluated and compared the SRA and BSW algorithms in their ability to model realistic 3-d LWC perturbation fields. Up to this point, our evaluations have been mainly qualitative, comparing the visual appearance of the fields and checking for the presence of artifacts.

We are also concerned with the flexibility of each algorithm to produce fields that are representative of a variety of cloud types. The Hurst and lacunarity parameters provide that flexibility in the SRA algorithm. Wavelength parameters control similar functions in the BSW, though we are limited to short wavelengths to avoid discontinuities and artifacts (see Section 2.2.3).

Future work will involve evaluating the turning bands algorithm with the same qualitative measures we have used with the SRA and BSW algorithms: field quality and algorithm flexibility. We will also evaluate the field algorithms based on more quantitative measures such as computational speed and memory requirements. Finally, we will compare LWC series produced with each of the algorithms to the LWC measurement data (part of Task 3).

### **4.4 INTEGRATION WITH OTHER SWOE MODELS**

The cloud scene simulation model is one of many models that will be used in the BTI/SWOE sensor evaluation program. Cloud model output fields will be used in both thermal and radiative transfer models developed independently. It is crucial that these varied models are compatible so that, for example, output from one model is of the correct type

and format to use as input to another. Task 5 deals explicitly with the question of SWOE compatibility and integration and is an important aspect of the modeling project.

Throughout model development we have carefully designed the cloud model around those specifications gathered early in the project during the requirements and analysis task (Task 1). When necessary, and in the absence of opinions from other SWOE users and modelers, we have made conservative design decisions, always keeping in mind the goal of developing a low-maintenance, modular model. In the upcoming months, as a part of Task 5, we will continue to solicit feedback from the SWOE community (especially in regard to the thermal and radiative transfer models) as we develop the enhanced cloud model.



## REFERENCES

1. Burger, C.F., and I.I. Gringorten, *Two-Dimensional Modeling for Lineal and Areal Probabilities of Weather Conditions*, AFGL-TR-84-0126, 1984, ADA147970.
2. Gringorten, I.I., and A.R. Boehm, *The 3D-BSW Model Applied to Climatology of Small Areas and Lines*, AFGL-TR-87-0251, 1987, ADA199114.
3. Peitgen, H.O., and D. Saupe, *The Science of Fractal Images*, Springer Verlag, New York, 1988.
4. Tompson, A.F.B., R. Ababou, and L.W. Gelhar, "Implementation of the Three-Dimensional Turning Bands Random Field Generator," *Water Resources Research*, Vol. 25, No. 10, October 1989, pp. 2227-2243.
5. Hutchison, K.D., and M.P. Ramos-Johnson, *Cloud Optical Properties Required by the SWOE Scene Models*, TASC Technical Information Memorandum TIM-6042-1, 1990.
6. Cianciolo, M.E., *Cloud Scene Simulation Model Version 1.0 User's Guide*, TASC Technical Information Memorandum TIM-6042-2, 1990.
7. Feddes, R.G., *A Synoptic-Scale Model for Simulating Condensed Atmospheric Moisture*, USAFETAC-TN-74-4, 1974.
8. Abramowitz, M., and I.A. Stegun, Eds., *Handbook of Mathematical Functions With Formulas, Graphs, and Mathematical Tables*, U.S. Department of Commerce, National Bureau of Standards, 10th printing 1972, pp. 932-933.
9. Parzen, E., *Stochastic Processes*, Holden-Day, Inc., San Francisco, 1962.
10. Cianciolo, M.E., *Cloud Scene Simulation Model Version 2.0 User's Guide*, TASC Technical Information Memorandum TIM-6042-3, 1991.
11. Lovejoy, S., "Area-Perimeter Relation for Rain and Cloud Areas," *Science*, 216, 1982, pp. 185-187.
12. Lovejoy, S., and B.B. Mandelbrot, "Fractal Properties of Rain and a Fractal Model," *Tellus*, 37A, 1985, pp. 209-232.
13. Cahalan, Robert F., and J.H. Joseph, "Fractal Statistics of Cloud Fields," *Monthly Weather Review*, Vol. 117, Feb. 1989, pp. 261-272.
14. Green, Robin M., *Spherical Astronomy*, Cambridge University Press, 1985.
15. Lorensen, W.E., and H.E. Cline, "Marching Cubes: A High Resolution 3D Surface Construction Algorithm," *ACM Computer Graphics SIGGRAPH 1987 Conference Proceedings*, Vol. 21, No. 4, July 1987, pp. 163-169.

## REFERENCES (Continued)

16. Foley, J.D., and A. Van Dam, *Fundamentals of Interactive Computer Graphics*, Addison-Wesley, Inc., 1982.
17. Glass, M., and D.D. Grantham, *Response of Cloud Microphysical Instruments to Aircraft Icing Conditions*, AFGL-TR-81-0192, 1981, ADA112317.